



10 CFR 50.55a

John J. Cadogan, Jr
Vice President,
Nuclear Engineering

102-06797-JJC/RKR/DCE
November 18, 2013

Palo Verde
Nuclear Generating Station
P.O. Box 52034
Phoenix, AZ 85072
Mail Station 7602
Tel 623 393 4083

ATTN: Document Control Desk
U.S. Nuclear Regulatory Commission
Washington, DC 20555-0001

Dear Sirs:

Subject: **Palo Verde Nuclear Generating Station (PVNGS)**
Unit 3
Docket No. 50-530
Response to Request for Additional Information - American
Society of Mechanical Engineers (ASME) Code, Section XI,
Request for Approval of an Alternative to Flaw Removal and
Characterization - Relief Request 51

Pursuant to 10 CFR 50.55a(a)(3)(i), Arizona Public Service Company (APS) requested the Nuclear Regulatory Commission (NRC) approve Relief Request 51, by letter number 102-06794, dated November 8, 2013 [Agencywide Documents Access and Management System (ADAMS) Accession No. ML13317A070]. APS proposed an alternative to the American Society of Mechanical Engineers (ASME) Boiler and Pressure Vessel Code, Section XI requirements related to axial flaw indications identified in a Unit 3 reactor vessel bottom mounted instrument (BMI) nozzle. Specifically, APS proposed a half-nozzle repair and a flaw evaluation as alternatives to the requirements for flaw removal of IWA-4421 and flaw characterization of IWA-3300.

By email dated November 15, 2013, the NRC staff provided a request for additional information (RAI). The enclosure to this letter contains the APS response to the NRC RAI.

No commitments are being made to the NRC by this letter.

A047

Enclosure

APS Response to Request for Additional Information (RAI) – Relief Request 51

Enclosure
APS Response to Response to (RAI) – Relief Request 51

Introduction

Pursuant to 10 CFR 50.55a(a)(3)(i) Arizona Public Service Company (APS) requested the Nuclear Regulatory Commission (NRC) approve Relief Request 51, by letter number 102-06794, dated November 8, 2013 [Agencywide Documents Access and Management System (ADAMS) Accession No. ML13317A070]. APS proposed an alternative to the ASME Code requirements of Section XI related to axial flaw indications identified in a Unit 3 reactor vessel bottom mounted instrument (BMI) nozzle. Specifically, APS proposed a half-nozzle repair and a flaw evaluation as alternatives to the requirements for flaw removal of IWA-4421 and flaw characterization of IWA-3300.

By email dated November 15, 2013, the NRC staff requested additional information (RAI). The APS responses to the NRC RAI items are provided in this enclosure.

List of Attachments

- Attachment 1 Thermal Stress during Loss of Secondary Pressure Transient in the Lower Head of Palo Verde Reactor Vessel

- Attachment 2 Dominion Engineering, Inc., Calculation No. C-7789-00-2, Revision No. 1, *Palo Verde Bottom Head Instrumentation Nozzle Stress Analysis*

NRC RAI-1

Section 4.1 of Attachment 2 [of Relief Request 51] reported that the nil-ductility reference temperature (RT_{NDT}) of -60 Degrees Fahrenheit ($^{\circ}F$) for the RPV bottom head [RVBH] is from Reference 1 of this Attachment. Please confirm that this value is from the Certified Material Test Report for the RVBH. If not, please justify the use of this RT_{NDT} value in this application.

APS Response

The RVBH is fabricated from two plates with different heat numbers. The RT_{NDT} value of -60 $^{\circ}F$ is from the Certified Material Test Reports (CMTRs) for the RVBH with an adjustment in accordance with ASME Code, Section III, Article NB-2331(a1), (a2), (a3), as provided in UFSAR Table 5.2-5B, "PVNGS Unit 3 Fracture Toughness Data Reactor Vessel (Plates)" as described below.

The CMTRs provide data for both Unit 3 RVBH plate material heat numbers and indicate that the drop weight NDT (T_{NDT}) is -70 $^{\circ}F$ for both heat numbers. In accordance with ASME Code, Section III, Article NB-2331, the RT_{NDT} is established as the greater of T_{NDT} and [$T_{CV} - 60^{\circ}F$], where T_{CV} is the temperature at which the specified Charpy Impact test requirements of NB-2331(a2) are met. From the CMTRs, the Charpy Impact test requirements are met at -10 $^{\circ}F$ for one heat number and 0 $^{\circ}F$ for the other. Based on the above, the RT_{NDT} was conservatively established as -60 $^{\circ}F$ (0 $^{\circ}F - 60^{\circ}F$) in accordance with NB-2331(a3).

NRC RAI-2

A typical flaw evaluation in accordance with the American Society of Mechanical Engineers Boiler and Pressure Vessel Code (ASME Code), Section XI requires consideration of emergency and faulted conditions in addition to the normal condition (e.g., Appendix A of the ASME Code, Section XI). The applied stresses for the flaw evaluation in Section 4.4 of Attachment 2 of Relief Request 51 are for the normal conditions only. Please address the flaw evaluation under the emergency and faulted conditions.

APS Response

Emergency and faulted conditions have been considered as described below, and were determined not to be significant to the results of the flaw evaluation.

Emergency Condition

The emergency condition is defined as the external piping loads applied to the BMI nozzle resulting from a postulated in-core instrumentation tubing leak. These thermal loads are applied to the new J-groove weld and weld pad at the relocated pressure boundary on the outer surface of the lower head. Since these loads would create

Enclosure
APS Response to Response to (RAI) – Relief Request 51

relatively minor stress changes at the inner surface of the lower head, they were not considered further in the current flaw evaluation of the remnant J-groove weld.

Faulted Conditions

The combined safe shutdown earthquake (SSE) and branch line pipe break (BLPB) represents one of two faulted conditions. These external loads are applied to the new J-groove weld and weld pad at the relocated pressure boundary on the outer surface of the lower head. Since these external loads would create relatively minor stresses at the inner surface of the lower head, they were not considered further in the current flaw evaluations of the remnant J-groove weld.

The second faulted condition is the loss of secondary pressure (LSP) transient described in the Palo Verde Updated Final Safety Analysis Report (UFSAR) Table 3.9.1-1. This transient is illustrated by the temperature and pressure time-history plots provided in Figure 1 of Attachment 1 to this enclosure.

The evaluation of this transient was performed in the same manner as the steady state (SS) + cooldown (CD) analysis submitted as part of the original submittal of Relief Request 51. The faulted condition stresses are added to the residual plus SS pressure and thermal stresses, as tabulated below. The maximum faulted condition, Loss of Secondary Pressure stresses, derived in Attachment 1 to this enclosure, occur at about 118 seconds into the transient (at the maximum through-wall temperature gradient) when the cold leg temperature is 344 °F and the pressure is less than 300 psia. It is therefore conservative to add the maximum thermal stresses for this transient to the SS pressure stresses.

Position x (in.)	SS	LSP	SS+LSP
	Hoop Stress		
	(ksi)	(ksi)	(ksi)
0.0000	50.014	46.34	96.35
0.2980	61.709	36.78	98.49
0.5950	73.123	28.35	101.48
0.8920	71.136	20.95	92.08
1.1890	74.007	14.50	88.50
1.4860	57.094	8.94	66.03
1.7830	24.199	4.21	28.41
2.0330	3.862	0.83	4.69
2.2460	40.983	-1.66	39.32

SS = Steady State
LSP = Loss of Secondary Pressure

Key portions of the flaw evaluations performed for the Residual + SS + CD normal condition stresses in Section 6-2 of Attachment 2 of Relief Request 51 are similarly provided here for the Residual + SS + Loss of Secondary Pressure faulted condition. The updated $K_I(a)$ stress intensity factor is 145.2 ksi√in. and the fracture toughness

Enclosure
APS Response to Response to (RAI) – Relief Request 51

margin is 1.39, which is just slightly below the code required value of 1.41. Therefore, the elastic plastic fracture mechanics (EPFM) flaw evaluation for the loss of secondary pressure transient is presented below with the appropriate safety factors for faulted conditions.

Ductile Crack Growth Stability Criterion:		$T_{app} < T_{mat}$							
At instability:		$T_{app} = T_{mat}$							
Safety Factors		KI_p^*	KI_s^*	$KI(a)$	a_e	$KI(a_e)$	J_{app}	T_{app}	Stable?
Primary	Secondary	(ksi√in)	(ksi√in)	(ksi√in)	(in.)	(ksi√in)	(kips/in)		
1.00	1.00	63.870	81.305	145.175	2.6334	163.625	0.882	3.025	Yes
1.25	1.00	79.838	81.305	161.143	2.7634	186.053	1.141	3.911	Yes
1.50	1.00	95.805	81.305	177.110	2.9071	209.735	1.450	4.970	Yes
5.00	1.00	319.350	81.305	400.655	6.3412	700.741	16.185	55.477	No
7.00	1.00	447.090	81.305	528.395	9.4968	1130.958	42.158	144.509	No
Iterate on safety factor until $T_{app} = T_{mat}$ to determine $J_{instability}$:									
							$J_{instability}$	T_{app}	T_{mat}
2.1737	2.1737	138.835	176.733	315.568	4.7208	476.215	7.475	25.622	25.622
at $J_{mat} = 1.450$ kips/in,		$T_{mat} = 184.170$		$(T_{app} - T_{mat} = 0.000)$					
Applied J-Integral Criterion:		$J_{app} < J_{0.1}$							
where,		$J_{0.1} = J_{mat}$ at $\Delta a = 0.1$ in.							
Safety Factors		KI_p^*	KI_s^*	$KI(a)$	a_e	$KI(a_e)$	J_{app}	$J_{0.1}$	OK?
Primary	Secondary	(ksi√in)	(ksi√in)	(ksi√in)	(in.)	(ksi√in)	(kips/in)	(kips/in)	
1.50	1.00	95.805	81.305	177.110	2.9071	209.735	1.450	2.701	Yes

The applied tearing modulus (T_{app}) of 4.970 is less than the material tearing modulus (T_{mat}) of 25.622 and the applied J-integral (J_{app}) of 1.450 kips/in is less than the material J-integral ($J_{0.1}$) of 2.701 kips/in at a flaw extension of 0.1 inch. Therefore, these results demonstrate that both EPFM acceptance criteria are satisfied using a safety factor of 1.5 for primary loads and 1.0 for secondary loads.

NRC RAI-3

Appendix A to Attachment 2 [of Relief Request 51] documented the thermal stresses during cooldown which were obtained using a 2-dimensional axisymmetric finite element model (FEM). The NRC staff needs further clarification regarding the FEM results to gain confidence in the FEM model:

- Please confirm that the results shown in Figures A-1 to A-5 and Table A-3 are 1-dimensional, i.e., the results (temperature and stresses) are the same for all points at inner diameter (ID), outer diameter (OD), or any surface that is defined by a specific depth of the RVBH. Demonstrate that the 1-dimensional results are realistic in this application.

APS Response

Yes, the results shown in Figures A-1 to A-5 and Table A-3 are 1-dimensional even though the model is constructed in 2-dimensions. The RVBH ID is exposed to the reactor coolant cooldown transient analyzed in Attachment 2 of Relief Request 51 (cooldown from T_c 565°F at 100°F/hr). The ID surfaces of the BMI nozzle halves are subject to a lesser cooldown rate when compared to the RVBH ID surface. The gap between the OD of the BMI nozzle halves and ID of the RVBH bore is filled with stagnant water. This limits heat transfer between the BMI nozzle halves and the RVBH wall. Since the boundary conditions and RVBH are symmetrical, the heat transfer in the RVBH is primarily in the radial direction. Accordingly, it is reasonable to simplify the thermal analysis as 1-dimensional.

- Please confirm that the temperature difference-time plot (right figure) in Figure A-2 is a plot of the maximum thermal gradient mentioned in Paragraph A.2 Item 4. If it is not, explain the significance of this parameter. Regardless of the confirmation, please identify the location (depth) where this temperature difference-time plot was obtained and explain the physical meaning of such a unique shape of the temperature difference-time plot.

APS Response

Yes, the temperature difference-time plot (right figure) in Figure A-2 is a plot of the maximum through wall temperature gradient for the RVBH, i.e., the plot of temperature difference (ID minus OD) of the modeled lower head noted as TEMP_4. The initial status of the entire lower head is assumed to have a uniform temperature of 565°F. During the 100°F/hr cooldown transient, the fluid bulk temperature of the reactor coolant drops to 70°F in 4.8 hours. Because the convection heat transfer coefficient at the inner surface of the lower head is much higher than that of the outer surface, the temperature on the inner surface drops faster than the outer surface at the beginning of the transient. After about 1.3 hours, the absolute value of the temperature difference reaches its maximum. After that, the temperature difference between ID and OD of the lower head starts to decrease and eventually approaches zero. After 4.8 hours, there is no further cooling of the inside surface and the temperature difference is driven by conduction from the warmer outer surface to the cooler inner surface. At a time point about 7 hours after the start of the cooldown transient, the lower head reaches a thermal balance at 70°F.

NRC RAI-4

Section 4.4 of Attachment 2 [of Relief Request 51] states, “Residual plus operating stresses are obtained from Reference [7].” Demonstrate that the residual stresses used in the flaw evaluation are consistent with what were approved by the NRC staff in

Enclosure

APS Response to Response to (RAI) – Relief Request 51

published safety evaluations (SEs), NUREGs, or other NRC documents. If this cannot be demonstrated, please provide Reference 7 to support this review.

APS Response

The requested Reference 7, Dominion Engineering, Inc., Calculation No. C-7789-00-2, Revision No. 1, *Palo Verde Bottom Head Instrumentation Nozzle Stress Analysis*, is provided in Attachment 2 of this enclosure. The document reports the results of a three dimensional elastic plastic finite element analysis (FEA) performed as part of a Westinghouse Owners Group (WOG) initiative on Bottom Mounted Instrument Nozzles related to WCAP 16468-NP, *Risk Assessment of Potential Cracking in Bottom Mounted Instrumentation Nozzles*, September 2005.

NRC RAI-5

Table 4-3 of Attachment 2 [of Relief Request 51] presents the hoop stresses at different depths of the RVBH wall for the steady state (SS), cooldown (CD), and their combined effect. The NRC staff has the following requests:

- Identify the loads that were considered in the SS condition (i.e., any of the three: pressure, steady state thermal load, and residual stresses). Repeat the similar identification for the CD condition.

APS Response

Attachment 2 of this enclosure provides the combined hoop and axial stresses from operating pressure, operating temperature and residual stresses.

The operating parameters used to represent the SS condition are as follows:

- Operating Pressure: 2235 pounds per square inch absolute (psia)
- Operating Temperature (Cold Leg Temperature): 565°F
- Weld residual stresses from FEA simulation (where the hoop stresses are bounding)

The parameters used to calculate the CD condition used the same total stresses as defined for the SS condition above and included a cooldown transient of 100°F/hour.

Enclosure

APS Response to Response to (RAI) – Relief Request 51

- Confirm that the thermal state associated with the SS condition is the starting point of the CD condition.

APS Response

The starting temperature is 565°F, which is the same value used for the normal operating temperature at steady state conditions for the RVBH (Cold Leg Temperature).

- The stress pattern for the SS condition (Column 2 of Table 4-3 under SS) is very unusual. Please provide the corresponding stress components due to pressure, thermal, and residual stresses for each position (or depth) in Table 4-3. Explain the unusual zigzag stress pattern to demonstrate that it is not caused by modeling errors.

APS Response

Attachment 2 of this enclosure does not provide each stress component separately. The total stress at each nozzle node location is shown along its vertical axis from the top to the bottom of the weld. Below the weld, the FEA provides nodal stresses at the nozzle as well as the lower head material. It is at this location that the lower head hoop stresses drop by a larger amount than the nozzle nodes because the weld no longer restrains the bore. The lower head hoop stresses then increase to provide equilibrium in the local region of the lower head. This is the reason for the unusual zigzag stress pattern.

To investigate the sensitivity of the results to the stress field, the EPFM flaw evaluations were repeated using only nozzle stresses for Column 2 of Table 4-3. In this manner, the value of the stress at the eighth position changed from 3.862 to 37.480 ksi and the last stress changed from 40.983 to 23.501 ksi. When only nozzle stresses are considered in the flaw evaluations, the applied J-integral changed from 0.953 to 1.002 kips/in and the applied tearing modulus changed from 17.508 to 18.405. This demonstrates that the final results are relatively insensitive to the stresses near the crack tip.

- If residual stresses are not included in the SS condition, confirm that residual stresses are considered in the subsequent applied stress intensity factor (K) or applied J calculations (Tables 6-1 and 6-2 do not show explicitly the contribution due to residual stresses).

APS Response

Residual stresses are considered in the SS condition, which is combined with the normal operating pressure and temperature in Attachment 2 of this enclosure, as described earlier in this RAI. This total stress is utilized in subsequent applied stress intensity factor (K) and applied J calculations in the fracture mechanics evaluation.

NRC RAI-6

Section 4.1.4 of Attachment 2 [of Relief Request 51] presents the generic J-R curve used in the elastic plastic fracture mechanics (EPFM) evaluation. This J-R curve is based on the J model from Appendix D to NUREG-0744, Vol. 2, Rev. 1, "Resolution of the Task A-11 Reactor Vessel Materials Toughness Safety Issue," 1982. The generic J-R curve models for various low upper-shelf RPV materials are presented in RG 1.161, "Evaluation of Reactor Pressure Vessels with Charpy Upper-Shelf Energy Less Than 50 FT-LB," 1995. Please provide J-R curves based on both approaches to demonstrate that your J-R curve based on NUREG-0744, Vol. 2, Rev. 1 is not significantly different from the RG 1.161 model. Provide correction and reassess your final conclusion if the difference is significant. Please note that the database underlying the J-R model for RPV base metals in RG 1.161 contains not just low upper-shelf energy materials.

APS Response

The EPFM flaw evaluations performed to demonstrate that a remnant flaw in the Palo Verde Nuclear Generating Station Unit 3 bottom mounted instrument nozzle number 3 is acceptable for one fuel cycle utilized methodology previously approved by the NRC for Arkansas Nuclear One Unit 1 (ML042890174), Watts Bar Unit 1 (ML073532246), and Davis Besse (ML102571569). These submittals were based on the same NUREG-0744 J-R curve correlation and the same EPFM safety factors that were used in the present submittal for Palo Verde, which are higher than those specified in Regulatory Guide 1.161.

The basic differences between the NUREG-744 and RG 1.161 approaches are the J-R correlations and the EPFM safety factors.

J-R Curve correlations for a Charpy upper shelf energy value of 119 ft-lbs:

NUREG-0744

$$J_{mat} = C(\Delta a)^m$$

$$C = 7.68$$

$$m = 0.45$$

RG 1.161

$$J_R = (MF) \{ C1 (\Delta a)^{C2} \exp[C3 (\Delta a)^{C4}] \}$$

$$C1 = \exp[-2.44 + 1.13 \ln(CVN) - 0.00277T]$$

$$C2 = 0.077 + 0.116 \ln(C1)$$

$$C3 = -0.0812 - 0.0092 \ln(C1)$$

$$C4 = -0.409$$

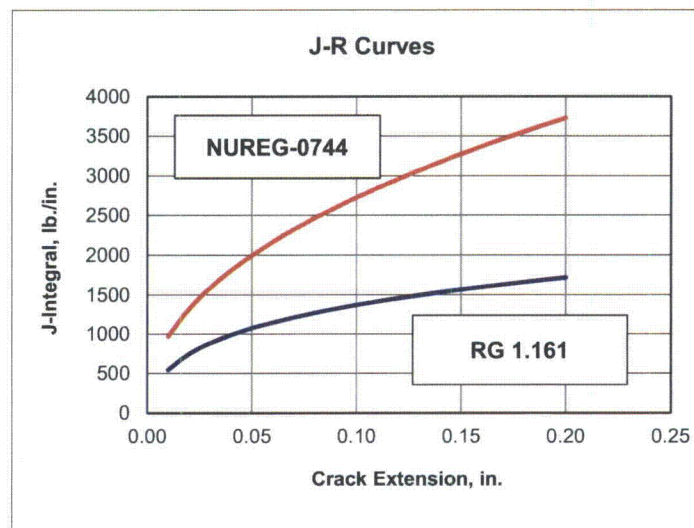
MF = Margin factor

APS Response to Response to (RAI) – Relief Request 51

At a temperature of T = 565 °F, the RG 1.161 J-R curve constants are:

- C1 = 4.0364
- C2 = 0.2389
- C3 = -0.0940
- C4 = -0.4090

Margin factors for the RG 1.161 approach are 0.749 for the Service Levels A (normal), B (upset), and C (emergency), and 1.0 for Service Level D (faulted). The following figure illustrates a lower J-integral resistance to ductile tearing curve provided by the RG 1.161 correlation for normal, upset, and emergency conditions compared to the NUREG-0744 correlation.



Equivalent safety factors are listed below for the two methodologies.

<u>Operating Conditions</u>	<u>Evaluation Method</u>	<u>Primary Loads</u>		<u>Secondary Loads</u>	
		<u>NUREG / RG</u>		<u>NUREG / RG</u>	
Normal conditions:	Limited flaw extension	1.5	1.4 ⁽¹⁾	1.0	1.0
	Stable flaw extension	3.0	1.5 ⁽²⁾	1.5	1.0
Faulted conditions:	Limited flaw extension	1.5	1.0	1.0	1.0
	Stable flaw extension	1.5	1.0	1.0	1.0

(1) Equivalent safety factor derived from 1.15 * 1.1 (ratio of maximum accumulation pressure*/design pressure) * ~1.1 (ratio of design pressure/operating pressure) = ~1.4

(2) Equivalent safety factor derived from 1.25 * 1.1 (ratio of maximum accumulation pressure*/design pressure) * ~1.1 (ratio of design pressure/operating pressure) = ~1.5

* Regulatory Guide 1.161 defines the maximum accumulation pressure as the value from the plant Overpressure Protection Report, but not exceeding 1.1 times the design pressure.

Enclosure
APS Response to Response to (RAI) – Relief Request 51

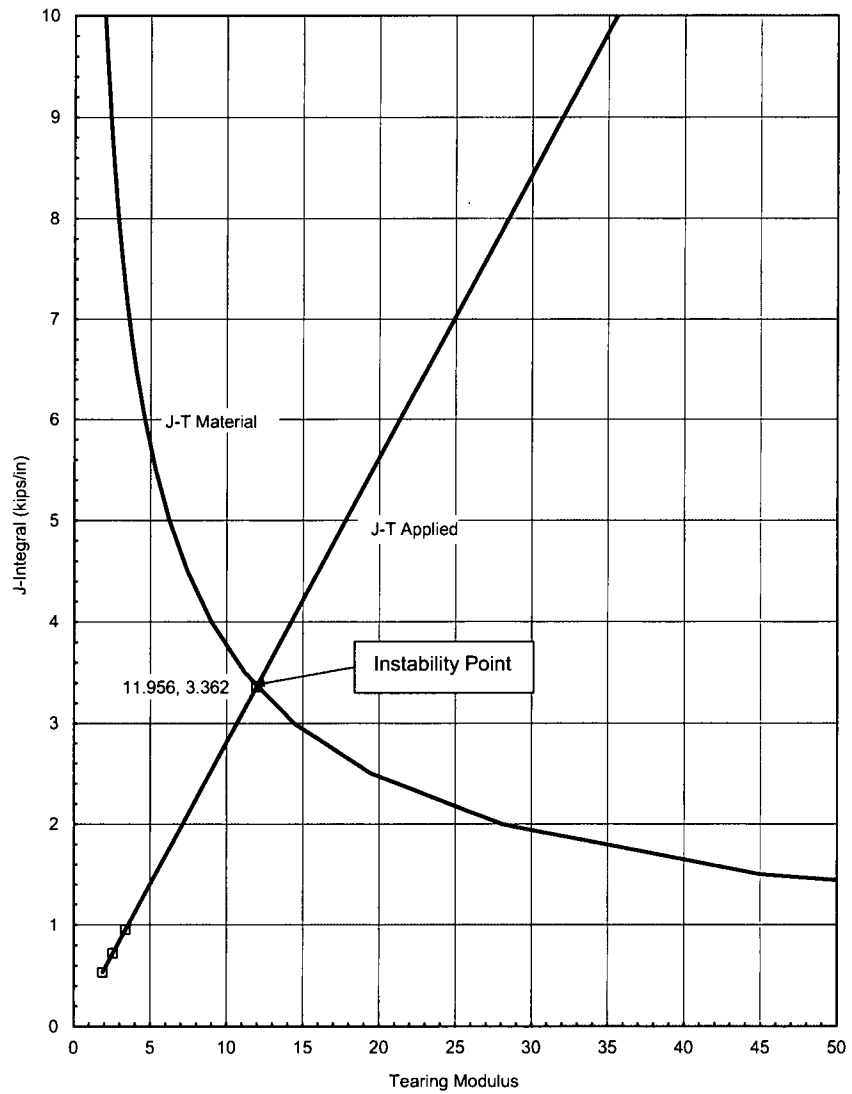
In order to address the different safety factors specified in the two standards, additional calculations have been performed using the complete RG 1.161 methodology (J-R curve and safety factors) to perform EPFM flaw evaluations for the residual + steady state + cooldown loads. In order to use the same analytical procedure for performing EPFM flaw evaluations, the RG 1.161 J-R curve is fitted to the same power law model that is used for the NUREG-0744 approach. The results of this evaluation are provided below:

EPFM Equations:		$J_{mat} = C(\Delta a)^m$	$C = 3.69$						
		$T_{mat} = (E/\sigma_f^2) * C_m(\Delta a)^{m-1}$	$m = 0.38$						
		$J_{app} = [K_I(a_e)]^2/E'$							
		$T_{app} = (E/\sigma_f^2) * (dJ_{app}/da)$							
Ductile Crack Growth Stability Criterion:		$T_{app} < T_{mat}$							
At instability:		$T_{app} = T_{mat}$							
Safety Factors		K_I^*p	K_I^*s	$K_I^*(a)$	a_e	$K_I'(a_e)$	J_{app}	T_{app}	Stable?
Primary	Secondary	(ksi√in)	(ksi√in)	(ksi√in)	(in.)	(ksi√in)	(kips/in)		
1.00	1.00	63.870	52.592	116.462	2.4733	127.209	0.533	1.897	Yes
1.25	1.00	79.838	52.592	132.429	2.5905	148.040	0.722	2.569	Yes
1.50	1.00	95.805	52.592	148.397	2.7229	170.073	0.953	3.390	Yes
5.00	1.00	319.350	52.592	371.942	6.1554	640.920	13.539	48.146	No
7.00	1.00	447.090	52.592	499.682	9.4411	1066.361	37.479	133.278	No
Iterate on safety factor until $T_{app} = T_{mat}$ to determine $J_{instability}$:									
2.0414	2.0414	130.386	107.362	237.748	3.7410	319.384	$J_{instability}$ 3.362	T_{app} 11.956	T_{mat} 11.956
at $J_{mat} = 0.953$ kips/in,		$T_{mat} = 94.708$		$(T_{app} - T_{mat} = 0.000)$					
Applied J-Integral Criterion:		$J_{app} < J_{0.1}$							
where,		$J_{0.1} = J_{mat}$ at $\Delta a = 0.1$ in.							
Safety Factors		K_I^*p	K_I^*s	$K_I^*(a)$	a_e	$K_I'(a_e)$	J_{app}	$J_{0.1}$	OK?
Primary	Secondary	(ksi√in)	(ksi√in)	(ksi√in)	(in.)	(ksi√in)	(kips/in)	(kips/in)	
1.40	1.00	89.418	52.592	142.010	2.6681	161.109	0.856	1.542	Yes

These results demonstrate that both EPFM acceptance criteria are satisfied using safety factors of 1.5 and 1.0 (primary and secondary) for stable flaw extension and 1.4 and 1.0 for limited flaw extension. The applied tearing modulus of 3.390 is less than the material tearing modulus of 11.956 (indicated in the J-T diagram on the following page) and the applied J-integral of 0.856 kips/in is less than the material J-integral of 1.542 kips/in at a flaw extension of 0.1 inch.

The results of this EPFM flaw evaluation demonstrate that using the J-R curve and safety factors in RG 1.161 confirms the acceptability of the current remnant flaw evaluations based on the NUREG-0744 material J-R curve and previously NRC approved safety factors.

Enclosure
APS Response to Response to (RAI) – Relief Request 51



J-T Diagram for EPFM Using Regulatory Guide 1.161

Enclosure
APS Response to Response to (RAI) – Relief Request 51

NRC RAI-7

Table 6-2 of Attachment 2 [of Relief Request 51] provides results for a number of parameters which were calculated during the EPFM evaluation. Please provide the flow stress σ_f at the operating temperature of 565 °F and a sample calculation for the applied tearing modulus T_{app} appeared in Column 9 of this table.

APS Response

The flow stress at 565 °F is 61.2 ksi, derived from the average of the minimum yield (42.4 ksi) and the minimum ultimate (80.0 ksi) strengths of the reactor vessel bottom head material. The applied tearing modulus with safety factors of 3 on primary loads and 1.5 on secondary loads, reported in Table 6-2 as 17.508, was calculated as follows:

Parameters	At Flaw Depth a	At Flaw Depth a - 0.01"	At Flaw Depth a + 0.01"	Units
a	2.073			in.
KI	116.46			ksi√in
KIp	63.87			ksi√in
Δa	0	-0.01	0.01	in.
E	27610			ksi
v	0.3			
$E' = E/(1-v^2)$	30341			ksi
σ_y	42.4			ksi
σ_u	80.0			ksi
$\sigma_f = 0.5*(\sigma_y + \sigma_u)$	61.2			ksi
a + Δa	2.073	2.063	2.083	in.
$KI = KI \sqrt{(a+\Delta a)/a}$	116.46	116.18	116.74	ksi√in
$KIp = KIp \sqrt{(a+\Delta a)/a}$	63.87	63.72	64.02	ksi√in
$KIt = KI - KIp$	52.59	52.46	52.72	ksi√in
SFp	3	3	3	
SFs	1.5	1.5	1.5	
$KI^*p = SFp KIp$	191.610	191.147	192.072	ksi√in
$KI^*s = SFs Kis$	78.888	78.697	79.078	ksi√in
$KI^* = KI^*p + KI^*s$	270.498	269.845	271.150	ksi√in
$ae = a + (1/6\pi) (KI^*/\sigma_f)^2$	4.2322	4.2118	4.2526	in.
$KI'(ae) = KI^* \sqrt{(ae)/a}$	386.50	385.57	387.43	ksi√in
$J_{app} = [KI'(ae)]^2 / E'$	4.923	4.900	4.947	kips/in
$T_{app} = (E/\sigma_f^2) [(J_{app}(a+\Delta a) - J_{app}(a-\Delta a))/2\Delta a]$	17.508			

ATTACHMENT 1

**THERMAL STRESS DURING LOSS OF SECONDARY PRESSURE TRANSIENT IN
THE LOWER HEAD OF PALO VERDE REACTOR VESSEL**

Thermal Stress during Loss of Secondary Pressure Transient in the Lower Head of Palo Verde Reactor Vessel

Purpose

The purpose of the analysis is to determine the maximum hoop thermal stress in the Palo Verde reactor vessel lower head developed during loss of secondary pressure transient in support of the response to RAI #2.

Methodology

1. Generate a 2D axisymmetric finite element model to simulate a simplified reactor vessel lower head with an inner radius of 93.3 inches and a thickness of 6.5 inches (Reference [A.1]);
2. Perform thermal transient analysis for loss of secondary pressure condition to determine the temperature field of the reactor vessel lower head;
3. Get temperature field and thermal gradients for each time point;
4. Identify maximum thermal gradient across thickness and the time point of its occurrence;
5. Perform structural analysis, using temperature field identified in Step 4, to determine the thermal stress distribution through the thickness of the lower head.

Assumptions

1. The finite element model represents a perfect hemisphere. Any feature other than the sphere portion of the base metal of the lower head, such as cladding, weld, and penetration elements are not included;
2. The fluid temperature data during Loss of Secondary Pressure transient are taken from Figure 5 of Reference [A.2] (see curve T_{COLD} in Figure 1). It has an approximately 22.5 °F/sec temperature drop rate during the first 100 seconds;
3. The initial condition of the lower head is assumed to be a uniformly distributed temperature of 565 °F.

Material Properties

Per Reference [A.1], the material of the reactor vessel lower head is SA-533 Gr. B Class 1 (C-Mn-Mo-0.4-0.7Ni). The material properties are taken from Reference [A.3] except the material densities are taken from Reference [A.5].

Table 1: Material Properties

Temp.	Modulus of Elasticity	Thermal Expansion Coefficient (α)	Thermal Conductivity (k)	Specific Heat (C)	Density (ρ)
°F	$\times 10^6$, psi	$\times 10^{-6}$, 1/°F	Btu/hr-in-°F	Btu/lb-°F	lb/in ³
100	29.80	6.13	2.5833	0.1147	0.2839
200	29.50	6.38	2.5000	0.1169	0.2831
300	29.00	6.60	2.4250	0.1210	0.2823
400	28.60	6.82	2.3417	0.1251	0.2817
500	28.00	7.02	2.2667	0.1292	0.2809
600	27.40	7.23	2.1833	0.1333	0.2802
700	26.60	7.44	2.1083	0.1393	0.2794
Reference	[A.3]	[A.3]	[A.3]	Calculated*	[A.5]

Note: $*C = K/(\rho \cdot T_d)$, where T_d is thermal diffusivity from the same source as thermal conductivity (k in the table).

Finite Element Model and Boundary Conditions and Results

Definition of the reactor coolant temperature history for Loss of Secondary Pressure transient is listed in Table 2 (see curve T_{COLD} in Figure 1 and Figure 5 of Reference [A.2]). The temperature data are input as bulk temperatures of the inner surface of the lower head in the thermal transient analysis.

Table 2: Reactor Coolant Temperature during Loss of Secondary Pressure Transient

Loss of Secondary Pressure Transient								
No.	Time (Sec)	Temp. (F)	No.	Time (Sec)	Temp. (F)	No.	Time (Sec)	Temp. (F)
1	0.00010	565.000	13	109.98600	343.322	25	255.06500	403.888
2	6.87838	464.089	14	118.69400	344.362	26	291.30900	406.988
3	14.58130	433.842	15	128.97200	349.265	27	324.68400	410.796
4	21.16600	413.791	16	132.03300	354.534	28	363.84200	414.595
5	25.18680	403.940	17	135.55700	364.369	29	403.01200	418.745
6	33.54480	394.082	18	136.68700	379.834	30	459.56400	423.919
7	41.89150	383.872	19	138.62900	374.215	31	519.01800	429.439
8	50.26070	374.365	20	144.57000	384.746	32	566.89600	434.629
9	62.97840	365.202	21	159.17400	389.291	33	601.68300	437.380
10	74.32940	358.502	22	181.01800	394.174	34	622.35200	495.703
11	89.96100	350.037	23	199.92500	397.656	35	639.72300	496.376
12	102.76900	343.687	24	223.14600	400.428			

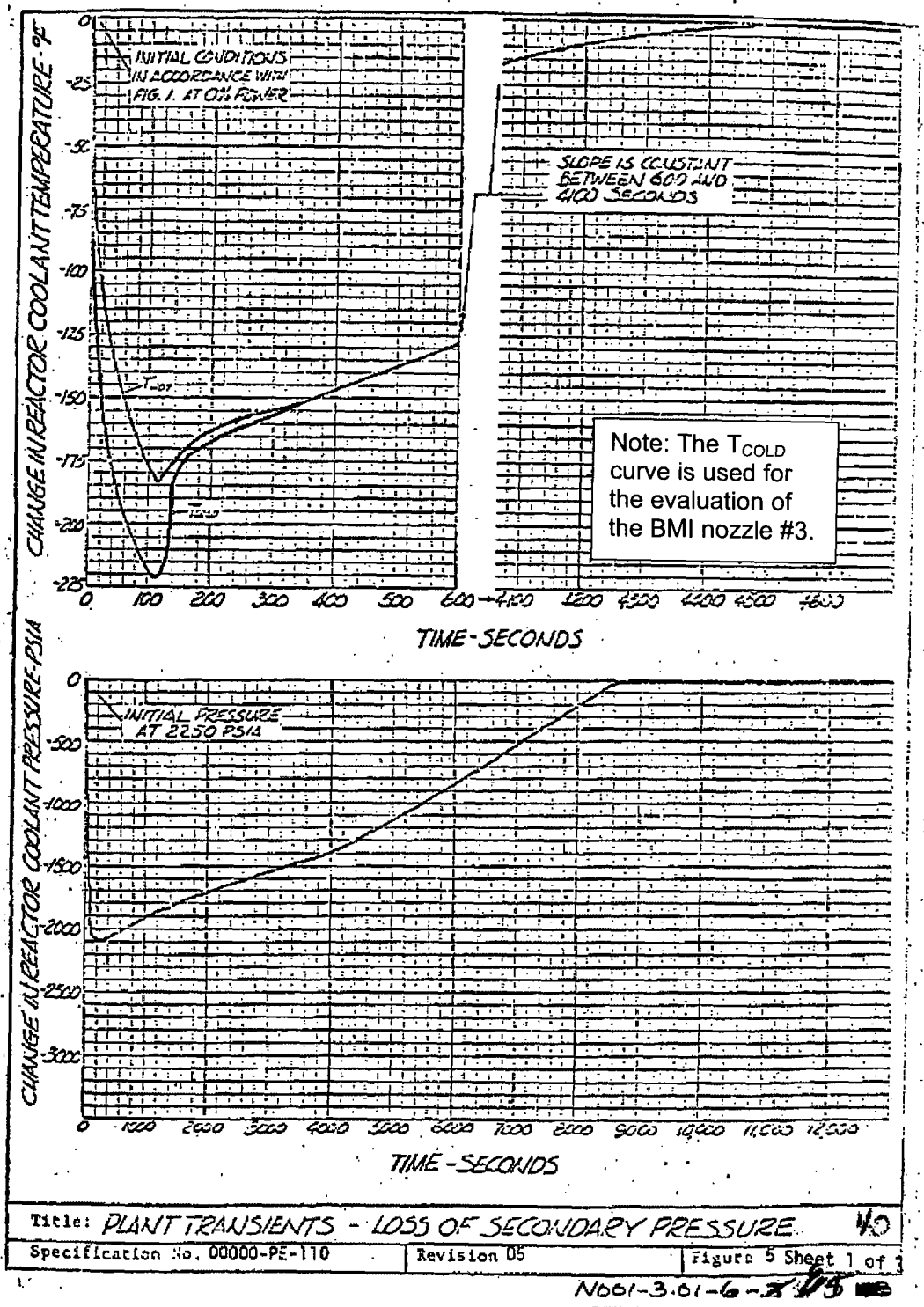


Figure 1: Plant Transient - Loss of Secondary Pressure

**Enclosure
APS Response to Response to (RAI) – Relief Request 51
Attachment 1**

A convection coefficient of 1000 Btu/hr-ft²-°F is applied on the inner surface of the base metal of the lower head. This value is based on experiences from similar projects performed in the past. The convection coefficient on the outer surface of the lower head is assumed to be 0.150 Btu/hr-ft²-°F and the ambient air temperature is assumed to be 70°F during Loss of Secondary Pressure transient. The lower head is assumed to be initially under uniformly distributed temperature of 565°F.

Figure 2 shows Finite element model boundary conditions and the temperature field. Figure 3 shows the history of temperature vs. time and the history of temperature gradient between inside and outside surface of the lower head vs. time. Note that curves identified with TEMP_1, TEMP_2 and TEMP_3 in the left graph of this figure are temperature histories for node located on inner surface, at depth of 1.5 inches from inner surface, and on outer surface. Figure 4 shows radial and hoop thermal stresses in the lower head at the maximum temperature difference time point during Loss of Secondary Pressure transient (at time of 0.032971 hours, i.e. 118.694 seconds). Table 3 lists radial and hoop thermal stresses in a path across the thickness of the lower head (path is shown in Figure 2). Figure 5 provides graphs for the thermal stresses vs. depth from ID to OD of the lower head. Figure 6 shows the temperature vs. depth from ID to OD.

It is seen that the maximum hoop thermal stress on the inner surface of the lower head during Loss of Secondary Pressure transient is about 46 ksi.

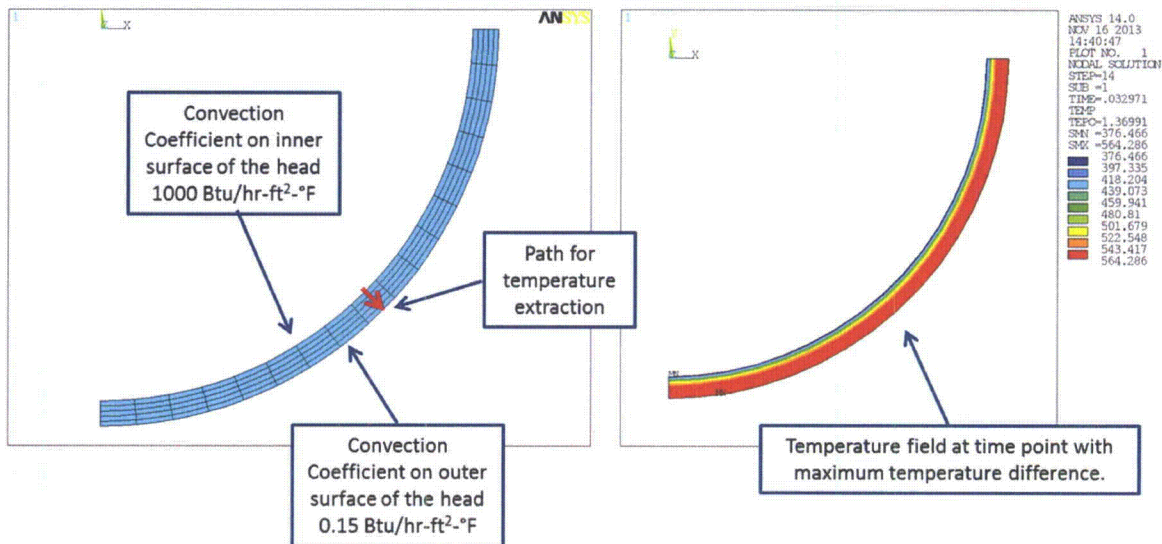


Figure 2: Finite Element Model, Boundary Condition (Left) and Temperature field (Right)

**Enclosure
APS Response to Response to (RAI) – Relief Request 51
Attachment 1**

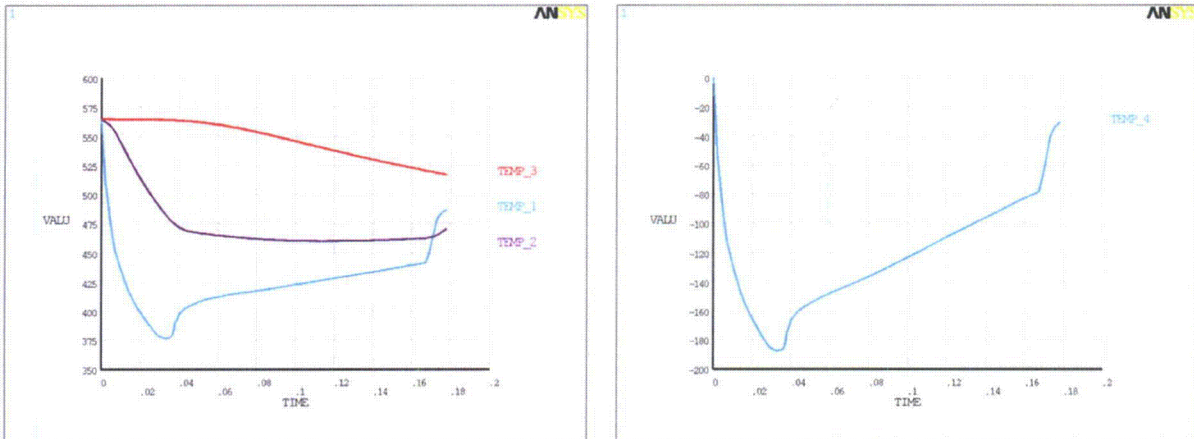


Figure 3: Temperature vs. Time (Left) and Temperature Difference vs. Time (Right)

Note: TEMP_1, TEMP_2, and TEMP_3 represents locations at inner surface, 1.5 inches from the inner surface, and the outer surface of the lower head, respectively. Units: °F for vertical axis, hours for horizontal axis.

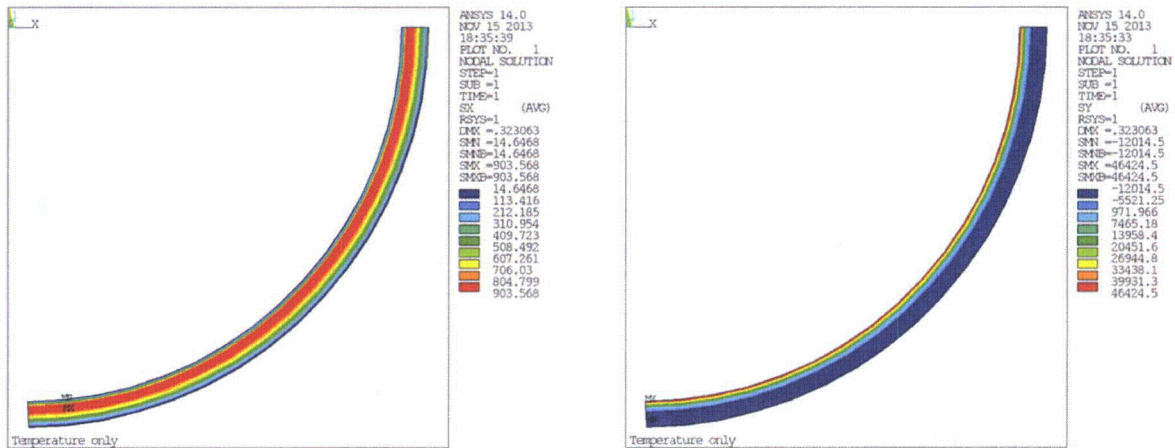


Figure 4: Thermal Stress in Radial (Left) and Hoop (Right) Directions

Note: Thermal stresses are calculated based on temperature field at the time point, during Loss of Secondary Pressure transient, with maximum temperature difference between ID and OD of the lower head.

**Enclosure
APS Response to Response to (RAI) – Relief Request 51
Attachment 1**

Table 3: Maximum Thermal Stresses in Lower Head during Loss of Secondary Pressure Transient

Palo Verde (Ri=93.35", Thk=6.5")			
Depth from ID to OD	Temperature (F)	SX* (psi)	SY* (psi), SZ* (psi)
0	377	17	46342
1.3	483	843	12365
2.6	539	903	-5281
3.9	559	655	-10908
5.2	564	335	-11999
6.5	564	16	-11950

Note: * The stresses are under spherical coordinate system. SX represents the stress in radial direction, and SY and SZ represent the stresses in the hoop directions.

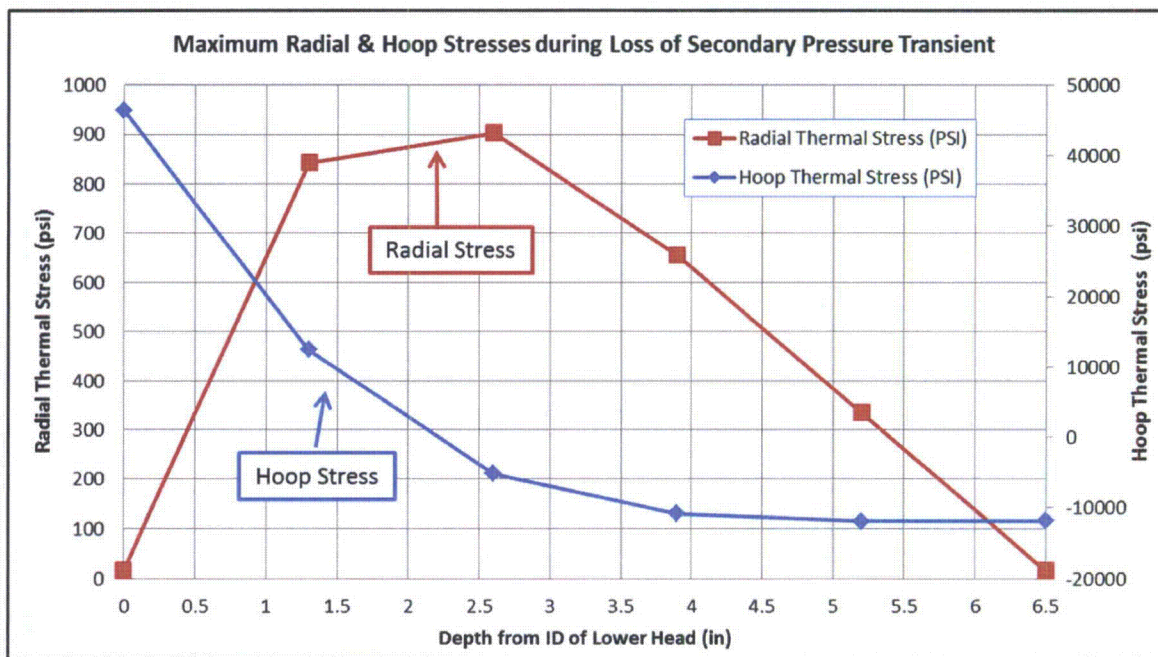


Figure 5: Thermal Stress in Radial (Left) and Hoop (Right) Directions vs. Depth from ID to OD

Note: Thermal stresses are calculated based on temperature field at the time point, during Loss of Secondary Pressure transient, with maximum temperature difference between ID and OD of the lower head.

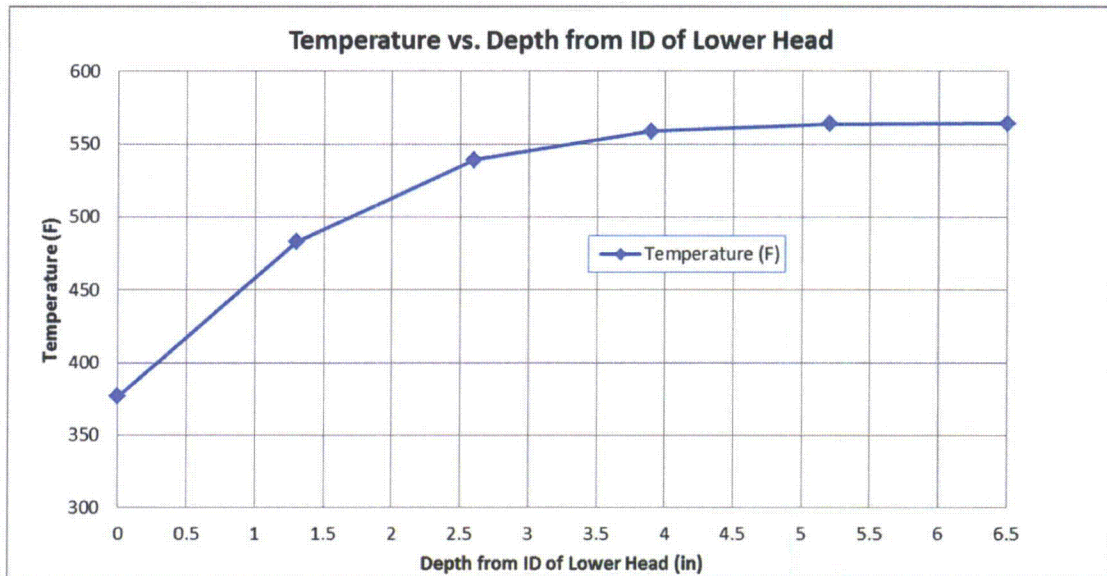


Figure 6: Temperature vs. Depth from ID to OD

Hardware, Software and Computer Files

Hardware and software

The EASI listed computer program ANSYS Release 14.0 (Reference [A.4]) is used in this calculation.

Verification tests of similar applications are listed as follows:

- Error notices for ANSYS Release 14.0 are reviewed and none apply for this analysis.
- Computer hardware used:
 - Dell Precision (Computer Name: MOCAO2, Service Tag #: 5VKT5S1) with Intel® Core™ i7-2640M CPU @ 2.80GHz, 2.80 GHz, 8.00 GB of RAM and Operating System is Microsoft Windows 7 Enterprise Version 2009 Service Pack 1.
 - Name of person running tests: Jasmine Cao
- Date of tests:
 - October 27, 2013 on computer “MOCAO2” (Service Tag #: 5VKT5S1)
- Acceptability: Results shown in files vm5.out and vm28.out show that the test runs are acceptable.

Computer Files

The computer files for the installation test have been stored in in the ColdStor under /cold/General-Access/32/32-9000000/32-9212942-000/official/ directory. The computer files for the thermal analysis are listed below:

Table 4: Computer Files

Name	Date modified	Type	Size
 LSP_tr.inp	11/15/2013 5:20 PM	INP File	8 KB
 post_pv_LSP.out	11/15/2013 5:22 PM	OUT File	14 KB
 rpv_pv_LSP.out	11/15/2013 5:22 PM	OUT File	154 KB

References

References identified with an (*) are maintained within [PVNGS3] Records System and are not retrievable from AREVA Records Management. These are acceptable references per AREVA Administrative Procedure 0402-01, Attachment 8.

- [A.1]. *Report N001-0301-00214, Revision 007, "Reactor Vessel, Unit 3, Analytical Report, V-CE-30869, 30AU84."
- [A.2]. *Customer Document, N001-0301-00006, Rev. 06, OEM Document No. 00000-PE-110, Rev. 05, B3, OEM Title "General Specification for Reactor Vessel Assembly."
- [A.3]. ASME Boiler and Pressure Vessel Code, Section III, Subsection NB, 1971 Edition, through Winter 1973 Addenda.
- [A.4]. ANSYS Finite Element Computer Code, Version 14.0, ANSYS Inc., Canonsburg, PA.
- [A.5]. AREVA Document NPGD-TM-500 Rev. D, "NPGMAT, NPGD Material Properties Program, User's Manual (03/1985)"

ATTACHMENT 2

**Dominion Engineering, Inc., Calculation No. C-7789-00-2, Revision
No. 1, *Palo Verde Bottom Head Instrumentation Nozzle Stress
Analysis***

DOMINION ENGINEERING, INC.

11730 PLAZA AMERICA DRIVE #310

RESTON, VIRGINIA 20190

Title: Palo Verde Bottom Head Instrumentation Nozzle Stress Analysis
 Task No.: 77-89 Calculation No.: C-7789-00-2 Revision No.: 1
 Page 1 of 13

Palo Verde Bottom Head Instrumentation Nozzle Stress Analysis

Record of Revisions				
Rev.	Description	Prepared by Date	Checked by Date	Reviewed by Date
0	Original Issue	M.R. Fleming 5/28/04	J.E. Broussard 5/28/04	J.E. Broussard 5/28/04
1	Added explicit statements in Sections 3 and 4 that head temperature and operating pressure are assumed values. Interchanged "above" and "below" in first paragraph of Section 5.2. Corrected figure/table descriptions in Section 5.3 to account for orientation of BMI nozzle penetration. Introduced Section 5.5 regarding QA control of software; added Reference 5. Changed "Top" to "Bottom" in title of Table 5-2. Corrected "Uphill" and "Downhill" labels in Table 5-4. Provided closer view of weld region in Figures 5-2 to 5.5. Corrected Figures 5-6 to 5-9; changed "Top" to "Bottom" in captions and corrected stress plot (now based on appropriate element selections per Westpost8). Replaced Westpost6 with Westpost8 in Attachment 2 (and Section 5.3).	 7/26/04	J.E. BROUSSARD 7/26/04	J.E. BROUSSARD 7/26/04

The last revision number to reflect any changes for each section of the calculation is shown in the Table of Contents. The last revision numbers to reflect any changes for tables and figures are shown in the List of Tables and the List of Figures. Changes made in the latest revision, except for Rev. 0 and revisions which change the calculation in its entirety, are indicated by a double line in the right hand margin as shown here.

DOMINION ENGINEERING, INC.

11730 PLAZA AMERICA DRIVE #310

RESTON, VIRGINIA 20190

Title: Palo Verde Bottom Head Instrumentation Nozzle Stress AnalysisTask No.: 77-89Calculation No.: C-7789-00-2Revision No.: 1Page 2 of 13

Table of Contents

<u>Sect.</u>		<u>Page</u>	<u>Last Mod. Rev.</u>
1.0	Purpose	4	0
2.0	Summary of Results	4	0
3.0	Input Requirements	4	1
4.0	Assumptions	5	1
5.0	Analysis	6	1
6.0	References	12	1

List of Tables

<u>Table No.</u>		<u>Last Mod. Rev.</u>
5-1	Nozzle Through Wall Hoop Stress at Selected Axial Locations	0
5-2	Nozzle Through Wall Axial Stress Along the Bottom of the Weld – Element-Oriented Coordinate System	1
5-3a	Nozzle ID and OD Hoop Stress (0.0° BMI Nozzle Case)	0
5-3b	Nozzle ID and OD Hoop Stress (26.6° BMI Nozzle Case)	0
5-3c	Nozzle ID and OD Hoop Stress (37.9° BMI Nozzle Case)	0
5-3d	Nozzle ID and OD Hoop Stress (49.0° BMI Nozzle Case)	0
5-4	Change in Inner Diameter at Selected Axial Locations	1

DOMINION ENGINEERING, INC.

11730 PLAZA AMERICA DRIVE #310

RESTON, VIRGINIA 20190

Title: Palo Verde Bottom Head Instrumentation Nozzle Stress AnalysisTask No.: 77-89Calculation No.: C-7789-00-2Revision No.: 1Page 3 of 13**List of Figures**

<u>Fig. No.</u>		<u>Last Mod.</u> <u>Rev.</u>
5-1	Bottom Head Instrumentation Nozzle Node Numbering Scheme	0
5-2	Operating Plus Residual Hoop (SY) and Axial (SZ) Stress (0.0° BMI Nozzle)	1
5-3	Operating Plus Residual Hoop (SY) and Axial (SZ) Stress (26.6° BMI Nozzle)	1
5-4	Operating Plus Residual Hoop (SY) and Axial (SZ) Stress (37.9° BMI Nozzle)	1
5-5	Operating Plus Residual Hoop (SY) and Axial (SZ) Stress (49.0° BMI Nozzle)	1
5-6	Operating Plus Residual Axial Stress at Bottom of Weld – Element-Oriented Coordinate 1 System – 0.0° BMI Nozzle	1
5-7	Operating Plus Residual Axial Stress at Bottom of Weld – Element-Oriented Coordinate 1 System – 26.6° BMI Nozzle	1
5-8	Operating Plus Residual Axial Stress at Bottom of Weld – Element-Oriented Coordinate 1 System – 37.9° BMI Nozzle	1
5-9	Operating Plus Residual Axial Stress at Bottom of Weld – Element-Oriented Coordinate 1 System – 49.0° BMI Nozzle	1

List of Attachments

<u>Att. No.</u>		<u>Last Mod.</u> <u>Rev.</u>
1	Palo Verde BMI Model Results Summaries	0
2	File "Westpost8.txt"	0

DOMINION ENGINEERING, INC.

11730 PLAZA AMERICA DRIVE #310

RESTON, VIRGINIA 20190

Title: Palo Verde Bottom Head Instrumentation Nozzle Stress AnalysisTask No.: 77-89Calculation No.: C-7789-00-2Revision No.: 1Page 4 of 13

1.0 Purpose

The purpose of this calculation is to document the results of finite element stress analyses of the Palo Verde bottom-mounted instrumentation (BMI) nozzle penetrations. In this analysis, a number of nozzle geometries spanning the range of BMI penetration angles in the Palo Verde reactor bottom head are investigated.

2.0 Summary of Results

Four BMI nozzle geometries were analyzed: the center penetration (0.0° nozzle), 26.6° nozzle, 37.9° nozzle, and outermost penetration (49.0° nozzle). The cases support the following conclusions:

1. The maximum nozzle ID hoop stresses are in the vicinity of the J-groove weld and are in excess of the corresponding axial stresses, suggesting that PWSCC cracking should be axially oriented.
2. Residual hoop stresses in the head shell region just beyond the J-groove weld are largely compressive.

3.0 Input Requirements

The following values are used in this calculation:

1. The local configuration of the J-groove weld attaching the BMI nozzles to the RPV bottom head. The details used for each model are taken from Combustion Engineering (CE) drawings (References 2a, 2c, 2f, 2h, 2k, 2m).
2. Detailed dimensions of the RPV bottom head and BMI nozzles. These values are taken from the set of CE drawings presented as Reference (2):

Nozzles:

- BMI Nozzle OD = 3.001 inches (in region of J-groove weld) – Ref. (2d, 2i, 2n)
- BMI Nozzle ID = 0.750 inches (in region of J-groove weld) – Ref. (2d, 2i, 2n)

Reactor Vessel:

- Cladding thickness = 0.16 inches – Ref. (2e, 2j)
- RPV Bottom Head Inner Radius (to cladding) = 93.19 inches – Ref. (2e, 2j)
- RPV Head Thickness (minimum, excluding cladding) = 6.5 inches – Ref. (2e, 2j)

4. Operating pressure and temperature. An operating temperature and pressure of 565°F and 2,235 psig were used for the current analysis. As is noted in Section 4, these values were assumed for this analysis.

DOMINION ENGINEERING, INC.

11730 PLAZA AMERICA DRIVE #310

RESTON, VIRGINIA 20190

Title: Palo Verde Bottom Head Instrumentation Nozzle Stress Analysis
Task No.: 77-89 Calculation No.: C-7789-00-2 Revision No.: 1
Page 5 of 13

4.0 Assumptions

The following modeling assumptions were used for the BMI nozzle modeling described in this calculation:

- 1. The range of clearance fits for the Palo Verde BMI nozzles may be calculated from References (2c) and (2d) (for Unit 1), (2h) and (2i) (for Unit 2), and (2m) and (2n) (for Unit 3). For the current analysis, the nominal 1.5 mil radial clearance fit was used.
2. Based on experimental stress-strain data and certified mill test report data for the materials listed below, the following room-temperature and 600°F elastic limit values were used in association with the elastic-perfectly plastic hardening laws described in Section 5.1:

Table with 3 columns: Material, 70°F, 600°F. Rows include Alloy 182 Welds (Original and Replacement), Low-Alloy Steel Shell, and Stainless Steel Cladding.

The elastic limit values for the base materials (head shell and cladding), which undergo small strains during the analysis, are based on the 0.2% offset yield strength for the material. The elastic limit values for the weld materials, which undergo large strains during the analysis, are based on an average of the reported yield and tensile strengths.

- 3. Based on high temperature yield strength data for Alloy 600 bar in Ref. (6), the following temperature scaling factors were applied to the Alloy 600 multi-linear isotropic hardening curve described in Section 5.1:
• 70 °F: 1.15 • 1,600 °F: 0.29
• 600 °F: 1.00 • 2,300 °F: 0.05
• 1,200 °F: 0.83 • 3,500 °F: 0.05
4. Prior to the J-groove welding process, a stress relief pass at 1,100°F is performed by applying a uniform temperature to the model. The stress-strain properties of the head, J-groove weld, and stainless cladding have been selected such that the low alloy steel material relaxes to a stress no greater than 25 ksi, while the other materials relax to stresses no greater than 30 ksi.
5. For the J-groove weld simulation, two passes of welding were performed: an inner pass and an outer pass. The model geometry was designed such that each weld pass is approximately the same volume.
6. The model geometries for each of the BMI nozzle cases were based on nominal as-designed dimensions. In addition, as noted in Section 3, the minimum dimensioned bottom head thickness (6.5 inches per Reference 2i) was used.
7. The BMI nozzle in each of the four cases was modeled such that the nozzle end (of length "D," as indicated in References 2d and 2h) at which the nozzle ID and OD are not equal to 0.750 and 3.001 inches is neglected. Omission of the nozzle end from the model is justified by the stress results presented in Figures 5-2 through 5-5, which show that both hoop (Sy) and axial (Sz) stresses decay

DOMINION ENGINEERING, INC.

11730 PLAZA AMERICA DRIVE #310

RESTON, VIRGINIA 20190

Title: Palo Verde Bottom Head Instrumentation Nozzle Stress AnalysisTask No.: 77-89Calculation No.: C-7789-00-2Revision No.: 1Page 6 of 13

rapidly in the nozzle over a very short distance from the top of the weld, such that nozzle stresses have reached negligible levels at the end of the modeled length. This rapid reduction in stress is attributable to the comparably stiff BMI nozzles at Palo Verde (due to the high wall thickness/diameter ratio of the nozzles).

8. Operating pressure and temperature. An operating temperature and pressure of 565°F and 2,235 psig, respectively, were assumed for the current analysis.

5.0 Analysis

5.1 *Finite Element Analyses*

Finite element analyses of the BMI nozzles were performed for a total of four cases, selected to bracket the range of BMI penetration angles in the Palo Verde reactor vessel heads. The four BMI geometry cases analyzed are: 0.0° (penetration no. 1), 26.6° (penetration nos. 21 and 22), 37.9° (penetration no. 41), and 49.0° (penetration nos. 60 and 61). Figure 5-1 shows the element geometry and node numbering scheme for the 37.9° BMI nozzle model. The numbering scheme used for the BMI model is identical for all four cases considered in this calculation.

ANSYS finite element analyses were performed using a model based on work developed for commercial customers and described in a 1994 EPRI report on the subject of PWSCC of Alloy 600 components in PWR primary system service (Ref. 1).

All nozzles were analyzed using 3D models. The model includes a sector of the alloy steel head with stainless steel cladding on the inside surface, the Alloy 600 nozzle, the Inconel buttering layer in the J-groove weld preparation (simulated as a single weld pass for this analysis), and the Inconel weld material divided into two "passes" of approximately equal volume. The stainless steel cladding and Inconel buttering layers were included in the model since these materials have significantly different coefficients of thermal conductivity compared to the carbon steel vessel head, and therefore influence the weld cooling process.

The boundary conditions on the conical surfaces are such that only radial deflections in the spherical coordinate system are permitted. The nozzles are modeled as being installed in holes in the vessel head using gap elements with an initial radial clearance of 1.5 mils (as discussed in Section 4.0).

DOMINION ENGINEERING, INC.

11730 PLAZA AMERICA DRIVE #310

RESTON, VIRGINIA 20190

Title: Palo Verde Bottom Head Instrumentation Nozzle Stress AnalysisTask No.: 77-89Calculation No.: C-7789-00-2Revision No.: 1Page 7 of 13

The current analysis model simulates the butter weld deposition process and the 1,100°F thermal stress relief of the head shell and butter (prior to J-groove welding). The butter weld deposition process is simulated using a single pass; i.e., the butter region is deposited as a single ring of material. After completion of the butter deposition step, the entire model (with the exception of the nozzle and J-groove weld elements, which are not yet active in the model) is uniformly raised to 1,100°F. As noted below, the elastic limit material properties of the head shell and butter at 1,100°F are reduced relative to those used in Reference (1) in order to simulate the stress relaxation caused by a multiple-hour stress relief at 1,100°F.

This analysis includes steps for weld depositing the butter and stress relieving the head and butter prior to the J-groove welding steps. In order to accurately model the stress relaxation in the weld region due to time at elevated temperature, the elastic limit for the Alloy 182 weld and stainless steel cladding at temperatures near 1,100°F are reduced relative to curves used in the Reference (1) analyses. The reduced elastic limits are set at values consistent with the lower residual stress levels brought about by the multiple-hour stress relief. This reduction in elastic limit allows stresses in the pressurizer shell, cladding, and buttering to redistribute at the lower residual stress levels.

The welds (both the weld butter and J-groove weld) are modeled as rings of weld metal which are heated and cooled. As noted above, weld buttering is simulated as a single weld pass; the J-groove weld is simulated as two weld passes. The welding process is simulated by combined thermal and structural analyses. The thermal analysis is used to generate nodal temperature distributions throughout the model at several points in time during the welding process. These nodal temperatures are then used as input conditions to the structural analysis, which calculates the thermally induced stresses. Once welding is completed, a hydrostatic pressure load is applied to, then removed from, the wetted regions of the model at ambient temperature. Finally, the model is loaded with operating temperature and pressure.

The combination of thermal and structural analyses required the use of both thermal and structural finite element types, as follows:

- Thermal Analysis. For the 3-D thermal analysis, eight-node thermal solids (SOLID70) and null elements (Type 0) were used. Use of null elements between the nozzle and head penetration has the effect of limiting heat transfer between the nozzle and head to conduction through the J-groove region. This assumption was made because the head penetrations are counterbored both at the upper and lower

DOMINION ENGINEERING, INC.

11730 PLAZA AMERICA DRIVE #310

RESTON, VIRGINIA 20190

Title: Palo Verde Bottom Head Instrumentation Nozzle Stress AnalysisTask No.: 77-89Calculation No.: C-7789-00-2Revision No.: 1Page 8 of 13

portions of the penetration, and because thermal communication between the surfaces that are nominally in contact was assumed to be poor.

- **Structural Analysis.** Eight-node 3-D isoparametric solid elements (SOLID45) and two-node interface elements (COMBIN40) were used for the 3-D structural analyses. The SOLID45 and COMBIN40 elements replaced the SOLID70 and null elements, respectively, which had been used for the thermal analysis. Degenerate four- and six-node solid elements were not used in areas of high stress gradient since they can lead to significant errors when used in these regions (7). Higher order elements were not used since they provide no greater accuracy for elastic-plastic analyses than the eight-node solids (7). Further details of the finite element modeling process are available in Reference (1).

In Reference (1), the analytical results of the finite element model were correlated with the experimental and field data that were available at the time. This study showed that the locations of observed cracking correlated well with regions of highest stress in the analytical model. Additionally, the measured ovality at EdF and Ringhals CRDM nozzles was found to correlate well with the analytically predicted ovality for these nozzles. Further details of the correlation between analytical and experimental/field data are available in Reference (1).

It is noted that the finite element model has been improved and refined since it was described in Reference (1). Among the improvements over the model described in Reference (1) are the following:

1. While the material properties used for the nozzle material continue to make use of multi-linear isotropic hardening, the material properties for the weld and weld buttering, head shell, and stainless steel cladding are now modeled using elastic-perfectly plastic hardening laws. Experience has shown that using multi-linear hardening properties in the analysis of materials that experience a high degree of plastic strain at elevated temperatures (such as those within the J-groove welds) results in significant work hardening once the material has cooled to lower temperatures. Using elastic-perfectly plastic hardening laws does not allow this artificial work hardening to occur, which yields more realistic stresses in the weld portions of the model.
2. The ability to refine the mesh in the various regions of the model. The model geometry used in this calculation makes use of approximately four times the mesh refinement in the J-groove weld areas as is shown in Reference (1), and uses greater mesh refinement in other areas of the model, such as the nozzle.

DOMINION ENGINEERING, INC.

11730 PLAZA AMERICA DRIVE #310

RESTON, VIRGINIA 20190

Title: Palo Verde Bottom Head Instrumentation Nozzle Stress AnalysisTask No.: 77-89Calculation No.: C-7789-00-2Revision No.: 1Page 9 of 13

3. The ability to perform four-pass welding, as an alternative to two passes. This feature produces more satisfactory results with J-groove welds that are deep compared to the wall thickness of the adjacent nozzle, such as for head vent and thermocouple RPV head penetrations.

In addition to these improvements, the finite element model has been modified for work specific to Westinghouse. In particular, the stress versus strain values for the multi-linear isotropic hardening used for the Alloy 600 nozzle material have been changed to be consistent with Alloy 600 cyclic stress-strain curve (CSSC) data obtained in Reference (3). The curve input for the analytical model is found in Figure 2-29 of (3), and is labeled "Reference Curve for Analysis." Because the CSSC curve in (3) is for only one temperature (600 °F), the reference curve was scaled to a number of other temperatures as follows. At each of the five strain values used to define the multi-linear isotropic hardening behavior of the nozzle material at 600 °F, the corresponding stress was linearly scaled up or down according to the scaling factors listed in Section 4.0, which are based on high temperature yield strength data for Alloy 600 in Reference (6). These scaling factors are consistent with the work performed using the version of the finite element model that is not specific to Westinghouse work. The ANSYS code that creates the finite element model with these changes has now been incorporated into DEI's "cirse.base" file. Version 2.4.6 of the cirse.base code was used for the four BMI cases considered in this calculation.

5.2 Analytical Results Summary

Summaries of the analytical results for each of the models analyzed are contained in Attachment 1 to this calculation. These summaries show the maximum hoop and axial stresses at the ID of the nozzle, at the "uphill" and "downhill" (closest to the center of the head) circumferential planes, as well as "below" the weld (axial portion of the nozzle including the weld region and extending through the head shell) and "above" the weld (axial portion of the nozzle extending into the RPV). Plots of the hoop (SY) and axial (SZ) stresses in each of the four BMI model cases are shown in Figures 5-2 through 5-5.

Figures 5-2 through 5-5 and Attachment 1 show that the maximum hoop stresses are in the vicinity of the J-groove weld, and are in excess of the corresponding axial stresses, suggesting that PWSCC cracking should be axially oriented. The results also show that operating plus residual stresses are influenced by penetration angle, with higher angles generally leading to higher maximum hoop and axial stresses.

DOMINION ENGINEERING, INC.

11730 PLAZA AMERICA DRIVE #310

RESTON, VIRGINIA 20190

Title: Palo Verde Bottom Head Instrumentation Nozzle Stress AnalysisTask No.: 77-89Calculation No.: C-7789-00-2Revision No.: 1Page 10 of 13

5.3 Additional Post-Processing of Analysis Results

In addition to the condensed post-processing included in Attachment 1 to this calculation, further post-processing was performed to determine the stresses and deflections at a number of other locations specified by Westinghouse personnel. The additional post-processing was performed using the file "Westpost8.txt," included as Attachment 2 to this calculation.

The results of the additional post-processing are presented in Tables 5-1 through 5-4 and in Figures 5-6 through 5-9. With the exception of Table 5-4, all data and stress plots are for the operating plus weld residual stress load condition. Table 5-1 presents the hoop stress distribution through the nozzle thickness at five specific axial locations for both the downhill and uphill sides of the nozzle. These locations are: 0.5" above the top of the weld, the top of the weld, the middle of the weld, the bottom of the weld, and 0.5" below the bottom of the weld. Table 5-2 presents the axial stress distribution through the nozzle thickness at the bottom of the weld, following the sweep of the weld from downhill to uphill. Data are tabulated for each of the nine circumferential planes in the model. For Table 5-2, the axial stress results are in an element-oriented coordinate system which follows the path of the weld; the axial stress results presented in Table 5-2 are normal to the path of the weld. Tables 5-3a through 5-3d present the hoop stress distribution along the ID and the OD of the four BMI nozzle geometries at both the downhill and uphill sides. Table 5-4 presents the weld residual deflection at the inner diameter of the nozzle at each of the nine circumferential planes in the model for four axial locations. These data are used to calculate the change in inner diameter at each of the locations. The four axial locations are presented as defined in Reference (4), and are as follows: Location 2 – 0.5" above the top of the uphill weld, Location 3 – top of the uphill weld, Location 4 – bottom of the uphill weld, and Location "X" – top of the downhill weld. Figures 5-6 through 5-9 are axial stress plots of the nozzle wall cross section at the bottom of the weld and following the sweep of the weld from uphill to downhill. As in Table 5-2, the stresses are in an element-oriented coordinate system which follows the path of the weld; the axial stress results presented are normal to the path of the weld.

5.4 Additional Files Stored Electronically

In addition to the condensed post-processing included in this calculation, more voluminous output results have been saved electronically in the following directories and filenames:

/data/t7789/PVB-0A/PVB-0A.nodelocs.txt

/data/t7789/PVB-0A/PVB-0A.results.txt

DOMINION ENGINEERING, INC.

11730 PLAZA AMERICA DRIVE #310

RESTON, VIRGINIA 20190

Title: Palo Verde Bottom Head Instrumentation Nozzle Stress AnalysisTask No.: 77-89Calculation No.: C-7789-00-2Revision No.: 1Page 11 of 13

/data/t7789/PVB-26A/PVB-26A.nodelocs.txt

/data/t7789/PVB-26A/PVB-26A.results.txt

/data/t7789/PVB-37A/PVB-37A.nodelocs.txt

/data/t7789/PVB-37A/PVB-37A.results.txt

/data/t7789/PVB-49A/PVB-49A.nodelocs.txt

/data/t7789/PVB-49A/PVB-49A.results.txt

These files (created using "Westpost6.txt"—see Attachment 2) have been transmitted to Westinghouse via e-mail and on CD-ROM on disk D-7789-00-1, Revision 0.

5.5 *Quality Assurance Software Controls*

The Palo Verde BMI nozzle analyses were performed on an HP J6700 workstation, under the HP-UX 11.0 operating system and ANSYS Revision 8.0, which is maintained in accordance with the provisions for control of software described in Dominion Engineering, Inc.'s (DEI's) quality assurance (QA) program for safety-related nuclear work (5).¹ In addition to QA controls associated with the procurement and use of the ANSYS software (e.g., maintenance of the ANSYS Inc. as an approved supplier of the software based on formal auditing and surveillance, formal periodic verification of ANSYS software installation), QA controls associated with all ANSYS batch input listings are also carried out by DEI. These include independent checks of a batch input listing each time it is used; review of all ANSYS Class 3 error reports and QA notices to assess their potential impact on a batch listing; and independent "check calculations" (e.g., comparison of model-computed nozzle and reactor vessel head stresses to theoretical closed-form solutions; confirmation that computed weld pass temperatures fell within target temperature ranges; and, for symmetric (0° nozzle angle) geometry cases, confirmation of the applied pressure loading and results symmetry) to ensure that the project-specific application of the analysis is appropriate. The review of ANSYS error reports and QA notices as well as the project-specific check calculations are documented formally in a QA memo to the project file (this project is DEI Task 77-89).

¹ DEI's quality assurance program for safety-related work (DEI-002) commits to applicable requirements of 10 CFR 21, Appendix B of 10 CFR 50, and ASME/ANSI NQA-1. This QA program is independently audited periodically by both NUPIC (the Nuclear Procurement Issues Committee) and NIAC (the Nuclear Industry Assessment Committee).

DOMINION ENGINEERING, INC.

11730 PLAZA AMERICA DRIVE #310

RESTON, VIRGINIA 20190

Title: Palo Verde Bottom Head Instrumentation Nozzle Stress AnalysisTask No.: 77-89Calculation No.: C-7789-00-2Revision No.: 1Page 12 of 13**6.0 References**

1. *PWSCC of Alloy 600 Materials in PWR Primary System Penetrations*, EPRI TR-103696, July 1994.
2. Combustion Engineering (CE) drawings of Palo Verde reactor vessel bottom head, nozzle and weld geometry (182.25" ID PWR):

Palo Verde Unit 1:

- a. CE Drawing E-78173-141-003, Revision 2, Lower Vessel Final Assembly
- b. CE Drawing E-78173-151-001, Revision 3, Bottom Head Welded Assembly
- c. CE Drawing E-78173-151-002, Revision 2, Bottom Head Penetrations
- d. CE Drawing E-78173-184-001, Revision 4, Bottom Head Instrument Tubes
- e. CE Drawing E-78173-171-003, Revision 7, General Arrangement

Palo Verde Unit 2:

- f. CE Drawing E-79173-141-003, Revision 1, Lower Vessel Final Assembly
- g. CE Drawing E-79173-151-001, Revision 4, Bottom Head Welded Assembly
- h. CE Drawing E-79173-151-002, Revision 1, Bottom Head Penetrations
- i. CE Drawing E-STD 11-184-033, Revision 4, Bottom Head Instrument Tubes
- j. CE Drawing E-79173-171-003, Revision 1, General Arrangement

Palo Verde Unit 3:

- k. CE Drawing E-65173-141-003, Revision 0, Lower Vessel Final Assembly
 - l. CE Drawing E-65173-151-001, Revision 1, Bottom Head Welded Assembly
 - m. CE Drawing E-65173-151-002, Revision 0, Bottom Head Penetrations
 - n. CE Drawing E-STD 11-184-033, Revision 4, Bottom Head Instrument Tubes
3. Ball, M. G., et al., "RV Closure Head Penetration Alloy 600 PWSCC," WCAP-13525, Revision 1, Westinghouse Electric Corporation, 1992.

DOMINION ENGINEERING, INC.

11730 PLAZA AMERICA DRIVE #310

RESTON, VIRGINIA 20190

Title: Palo Verde Bottom Head Instrumentation Nozzle Stress AnalysisTask No.: 77-89Calculation No.: C-7789-00-2Revision No.: 1Page 13 of 13

4. Incoming Correspondence IC-7736-00-3, Fax from Warren Bamford (Westinghouse) to John Broussard (Dominion Engineering, Inc.) defining diameter measurement elevations, dated January 8, 2002. (Note: This document was transmitted to DEI in support of work performed for Task 7736 and is filed in the Task 77-36 Project File.)
5. *Dominion Engineering, Inc. Quality Assurance Manual for Safety-Related Nuclear Work*, DEI-002, March 30, 2004.
6. *Properties and Selection: Stainless Steels, Tool Materials, and Special-Purpose Metals*, ASM Materials Handbook Volume 3, Ninth Edition, p. 218, 1980.
7. "Modeling and Meshing Guide," ANSYS 8.0 Documentation, ANSYS, Inc.

Table 5-1

Nozzle Through Wall Hoop Stress at Selected Axial Locations

Nozzle Angle	Percent Through Wall	Downhill Side Hoop Stress (psi)					Uphill Side Hoop Stress (psi)				
		0.5" Above Weld	Top of Weld	Middle of Weld	Bottom of Weld	0.5" Below Weld	0.5" Above Weld	Top of Weld	Middle of Weld	Bottom of Weld	0.5" Below Weld
0.0	ID	-13,785	-22,532	3,690	14,725	21,851	-13,785	-22,532	3,690	14,725	21,851
0.0	13%	-10,954	-16,817	3,287	12,880	16,738	-10,954	-16,817	3,287	12,880	16,738
0.0	25%	-8,129	-10,764	3,571	15,636	14,306	-8,129	-10,764	3,571	15,636	14,306
0.0	38%	-5,627	-4,115	7,066	20,683	15,549	-5,627	-4,115	7,066	20,683	15,549
0.0	50%	-3,051	6,517	15,457	27,495	20,932	-3,051	6,517	15,457	27,495	20,932
0.0	63%	506	21,110	29,941	34,945	29,239	506	21,110	29,941	34,945	29,239
0.0	75%	4,150	36,194	50,007	45,980	30,834	4,150	36,194	50,007	45,980	30,834
0.0	88%	5,567	49,807	66,371	53,320	25,883	5,567	49,807	66,371	53,320	25,883
0.0	OD	4,627	50,014	71,136	24,199	23,501	4,627	50,014	71,136	24,199	23,501
26.6	ID	28,436	33,371	32,823	34,545	13,336	-4,885	-17,537	4,051	17,454	33,997
26.6	13%	21,943	25,422	31,560	30,609	7,624	-3,168	-12,577	8,001	15,315	23,645
26.6	25%	19,303	23,018	33,841	33,657	7,544	-2,670	-9,997	11,687	16,509	19,479
26.6	38%	18,959	24,180	36,204	38,896	9,804	-3,213	-6,705	16,393	18,479	18,093
26.6	50%	21,399	29,721	41,373	45,536	12,310	-3,979	1,468	23,807	23,652	19,803
26.6	63%	25,111	41,869	51,155	53,468	14,254	-4,907	17,001	33,269	29,996	24,913
26.6	75%	27,889	53,913	64,951	58,250	12,594	-5,801	32,050	45,804	42,756	33,263
26.6	88%	24,312	62,486	69,723	55,093	6,171	-6,269	43,321	55,175	39,909	43,541
26.6	OD	23,084	59,897	68,511	45,873	2,368	-9,486	39,386	59,288	2,734	48,174
37.9	ID	43,700	41,628	43,308	22,896	8,496	-3,299	-14,779	497	24,164	40,322
37.9	13%	33,720	35,393	41,289	18,700	2,371	-3,762	-11,034	5,395	18,608	29,175
37.9	25%	29,650	36,295	45,524	21,752	1,843	-4,510	-11,124	11,161	19,654	23,475
37.9	38%	29,230	37,927	49,070	26,647	3,042	-5,554	-10,863	18,046	21,264	20,742
37.9	50%	30,675	41,823	55,978	34,044	3,897	-6,533	-4,062	27,288	25,452	21,267
37.9	63%	35,377	49,496	66,014	43,807	4,576	-7,572	13,282	37,834	30,770	23,541
37.9	75%	40,949	57,373	77,036	50,263	823	-8,607	32,053	48,996	41,816	29,216
37.9	88%	47,721	59,023	75,126	47,473	-10,570	-9,183	36,231	52,487	30,749	34,317
37.9	OD	43,538	48,004	67,306	53,576	-18,301	-12,435	28,012	52,298	-1,327	34,890
49.0	ID	52,035	54,862	46,672	13,099	3,968	-4,271	-14,636	-5,445	29,289	44,282
49.0	13%	41,307	46,038	42,751	8,050	-2,553	-3,430	-11,770	1,033	18,711	31,099
49.0	25%	38,179	47,341	46,966	9,663	-3,051	-4,050	-14,478	7,740	19,185	24,444
49.0	38%	36,873	48,094	50,819	13,829	-1,315	-5,010	-15,617	16,413	22,231	20,904
49.0	50%	36,936	51,194	58,318	20,814	-209	-6,060	-8,234	27,662	25,663	20,136
49.0	63%	38,509	55,154	67,620	28,630	-552	-7,040	9,937	39,024	29,432	19,491
49.0	75%	39,441	57,180	74,629	37,256	-5,634	-7,613	31,203	46,212	37,072	21,984
49.0	88%	40,196	51,830	68,347	35,242	-19,341	-8,261	30,597	45,334	22,477	17,036
49.0	OD	33,717	37,236	61,176	46,778	-30,370	-10,584	17,751	48,644	-846	12,297

Note: Nozzle yield strength at 600°F operating temperature is 39.3 ksi.

Table 5-2

Nozzle Through Wall Axial Stress Along the Bottom of the Weld -- Element-Oriented Coordinate System

Nozzle Angle	Percent Through Wall	Local Axial Stress (psi) at Circumferential Location								
		Downhill -90°	-67.5°	-45°	-22.5°	0°	22.5°	45°	67.5°	Uphill 90°
0.0	ID	-35,191	-35,191	-35,192	-35,192	-35,192	-35,192	-35,192	-35,191	-35,191
0.0	13%	-36,030	-36,030	-36,030	-36,030	-36,030	-36,030	-36,030	-36,030	-36,030
0.0	25%	-32,602	-32,602	-32,602	-32,602	-32,602	-32,602	-32,602	-32,602	-32,602
0.0	38%	-28,709	-28,709	-28,708	-28,708	-28,708	-28,708	-28,708	-28,709	-28,709
0.0	50%	-23,744	-23,744	-23,743	-23,743	-23,743	-23,743	-23,743	-23,744	-23,744
0.0	63%	-15,472	-15,474	-15,472	-15,472	-15,472	-15,472	-15,472	-15,474	-15,472
0.0	75%	-3,073	-3,074	-3,071	-3,072	-3,072	-3,072	-3,071	-3,074	-3,073
0.0	88%	15,477	15,476	15,478	15,477	15,477	15,477	15,478	15,476	15,477
0.0	OD	5,743	5,739	5,739	5,740	5,740	5,740	5,739	5,739	5,743
26.6	ID	16,455	18,431	18,105	10,848	3,528	-1,815	-6,234	-14,229	-20,455
26.6	13%	10,611	10,577	9,478	4,289	-1,138	-5,508	-9,781	-17,664	-23,646
26.6	25%	5,134	4,458	3,109	-576	-4,619	-8,338	-12,149	-18,699	-23,267
26.6	38%	2,417	1,167	-321	-3,391	-6,722	-9,573	-12,375	-17,579	-21,088
26.6	50%	2,690	688	-1,315	-4,237	-6,630	-8,249	-9,917	-13,536	-15,970
26.6	63%	1,760	-37	-1,777	-2,942	-3,004	-3,047	-3,995	-6,962	-9,001
26.6	75%	1,962	615	275	917	3,530	6,644	8,501	7,775	6,913
26.6	88%	14,001	13,619	14,127	15,626	20,165	27,803	31,348	29,932	27,982
26.6	OD	9,472	8,712	9,735	11,435	11,385	9,411	5,877	3,298	1,353
37.9	ID	22,467	27,881	30,808	21,920	8,676	419	-935	-243	-1,120
37.9	13%	18,847	21,064	21,928	15,838	6,593	-675	-2,747	-4,691	-7,554
37.9	25%	15,116	15,755	15,308	10,770	4,290	-1,342	-3,254	-6,015	-8,560
37.9	38%	13,422	12,308	10,711	7,022	1,970	-2,234	-3,203	-5,848	-7,761
37.9	50%	13,266	10,371	7,997	4,640	676	-1,708	-1,298	-2,792	-3,761
37.9	63%	11,114	7,255	5,103	3,043	2,237	2,241	3,572	2,605	1,891
37.9	75%	9,782	5,652	3,664	2,951	6,095	10,311	14,452	15,495	16,117
37.9	88%	11,902	12,619	14,340	16,242	22,340	31,713	35,991	32,700	30,255
37.9	OD	14,345	13,454	11,893	13,226	13,497	11,057	7,472	4,207	1,092
49.0	ID	15,395	22,427	31,115	23,697	2,729	-7,304	-3,268	8,877	14,330
49.0	13%	12,338	16,144	22,301	19,687	6,300	-3,359	-1,519	3,811	3,958
49.0	25%	11,846	14,153	17,206	14,008	5,885	-999	206	3,573	4,689
49.0	38%	13,189	13,501	13,949	9,774	4,325	-494	1,013	4,270	6,413
49.0	50%	15,885	14,390	12,262	7,541	3,275	233	3,374	7,087	9,644
49.0	63%	16,391	12,615	9,035	5,557	3,919	4,348	8,349	12,178	14,454
49.0	75%	11,598	8,380	5,611	3,326	6,849	13,168	18,939	22,891	24,867
49.0	88%	5,484	7,941	10,517	13,606	22,285	35,276	37,657	32,909	29,861
49.0	OD	13,455	12,549	9,628	12,680	12,378	11,107	6,970	2,668	-2,693

Table 5-3a

Nozzle ID and OD Hoop Stress (0.0° BMI Nozzle Case)

	Downhill Side				Uphill Side			
	Nodes	Axial Height	ID Hoop Stress (psi)	OD Hoop Stress (psi)	Nodes	Axial Height	ID Hoop Stress (psi)	OD Hoop Stress (psi)
Nozzle Top	80001, 80009	0.00	16,457	7,289	1, 9	0.00	16,457	7,289
	80101, 80109	0.30	1,701	5,111	101, 109	0.30	1,701	5,111
	80201, 80209	0.54	-13,785	4,627	201, 209	0.54	-13,785	4,627
	80301, 80309	0.73	-22,054	6,339	301, 309	0.73	-22,054	6,339
	80401, 80409	0.88	-25,439	22,325	401, 409	0.88	-25,439	22,325
	80501, 80509	1.01	-25,618	35,694	501, 509	1.01	-25,618	35,694
Weld Top	80601, 80609	1.11	-22,532	50,014	601, 609	1.11	-22,532	50,014
	80701, 80709	1.40	-6,979	61,709	701, 709	1.40	-6,979	61,709
	80801, 80809	1.70	4,693	73,123	801, 809	1.70	4,693	73,123
	80901, 80909	2.00	3,690	71,136	901, 909	2.00	3,690	71,136
	81001, 81009	2.29	4,615	74,007	1001, 1009	2.29	4,615	74,007
	81101, 81009	2.59	8,205	57,094	1101, 1009	2.59	8,205	57,094
Weld Bottom	81201, 81209	2.89	14,725	24,199	1201, 1209	2.89	14,725	24,199
	81301, 81309	3.14	18,147	37,480	1301, 1309	3.14	18,147	37,480
	81401, 81409	3.35	21,851	23,501	1401, 1409	3.35	21,851	23,501
	81501, 81509	3.61	20,231	13,797	1501, 1509	3.61	20,231	13,797
	81601, 81609	3.91	9,738	6,732	1601, 1609	3.91	9,738	6,732
	81701, 81709	4.27	6,103	1,736	1701, 1709	4.27	6,103	1,736
	81801, 81809	4.71	4,382	912	1801, 1809	4.71	4,382	912
	81901, 81909	5.23	3,118	206	1901, 1909	5.23	3,118	206
	82001, 82009	5.85	2,527	202	2001, 2009	5.85	2,527	202
	82101, 82109	6.60	2,446	228	2101, 2109	6.60	2,446	228
	82201, 82209	7.48	2,505	274	2201, 2209	7.48	2,505	274
	82301, 82309	8.55	2,526	281	2301, 2309	8.55	2,526	281
	82401, 82409	9.30	2,528	280	2401, 2409	9.30	2,528	280
Nozzle Bottom	82501, 82509	10.06	2,499	277	2501, 2509	10.06	2,499	277

Table 5-3b

Nozzle ID and OD Hoop Stress (26.6° BMI Nozzle Case)

	Downhill Side				Uphill Side			
	Nodes	Axial Height	ID Hoop Stress (psi)	OD Hoop Stress (psi)	Nodes	Axial Height	ID Hoop Stress (psi)	OD Hoop Stress (psi)
Nozzle Top	80001, 80009	0.00	-2,426	-2,223	1, 9	0.00	3,125	-2,523
	80101, 80109	0.83	-2,672	-298	101, 109	0.27	162	-3,897
	80201, 80209	1.50	-10,206	4,112	201, 209	0.49	-4,885	-9,486
	80301, 80309	2.03	5,781	10,010	301, 309	0.66	-12,518	-10,675
	80401, 80409	2.46	28,436	23,084	401, 409	0.80	-16,477	5,995
	80501, 80509	2.80	34,552	48,931	501, 509	0.91	-17,755	28,534
Weld Top	80601, 80609	3.07	33,371	59,897	601, 609	1.00	-17,537	39,386
	80701, 80709	3.35	29,802	68,922	701, 709	1.31	-14,008	66,712
	80801, 80809	3.63	30,558	67,159	801, 809	1.62	-3,563	73,838
	80901, 80909	3.91	32,823	68,511	901, 909	1.93	4,051	59,288
	81001, 81009	4.19	36,388	78,814	1001, 1009	2.24	8,021	39,518
	81101, 81009	4.47	38,921	60,206	1101, 1009	2.55	8,709	20,376
Weld Bottom	81201, 81209	4.74	34,545	45,873	1201, 1209	2.86	17,454	2,734
	81301, 81309	4.99	22,180	20,541	1301, 1309	3.11	29,151	29,529
	81401, 81409	5.17	13,336	2,368	1401, 1409	3.34	33,997	48,174
	81501, 81509	5.40	5,200	-3,461	1501, 1509	3.62	35,655	21,802
	81601, 81609	5.68	-776	2,634	1601, 1609	3.96	31,781	8,542
	81701, 81709	6.02	1,056	-150	1701, 1709	4.37	22,421	1,559
	81801, 81809	6.45	2,194	502	1801, 1809	4.86	3,972	-292
	81901, 81909	6.97	2,648	395	1901, 1909	5.45	544	-170
	82001, 82009	7.63	2,819	589	2001, 2009	6.16	2,254	457
	82101, 82109	8.43	3,380	-948	2101, 2109	7.01	2,731	458
	82201, 82209	9.43	4,173	-3,181	2201, 2209	8.04	2,935	304
	82301, 82309	10.66	4,433	-5,339	2301, 2309	9.28	3,522	199
	82401, 82409	11.42	3,548	1,180	2401, 2409	10.73	3,666	208
	Nozzle Bottom	82501, 82509	12.18	2,828	56	2501, 2509	12.18	2,874

Table 5-3c

Nozzle ID and OD Hoop Stress (37.9° BMI Nozzle Case)

	Downhill Side				Uphill Side			
	Nodes	Axial Height	ID Hoop Stress (psi)	OD Hoop Stress (psi)	Nodes	Axial Height	ID Hoop Stress (psi)	OD Hoop Stress (psi)
Nozzle Top	80001, 80009	0.00	-3,564	-2,603	1, 9	0.00	651	-3,725
	80101, 80109	1.12	-3,571	-1,919	101, 109	0.25	-2,555	-6,490
	80201, 80209	2.02	730	703	201, 209	0.46	-3,299	-12,435
	80301, 80309	2.74	30,410	7,583	301, 309	0.62	-7,476	-10,789
	80401, 80409	3.31	43,165	21,810	401, 409	0.75	-11,690	2,576
	80501, 80509	3.77	43,700	43,538	501, 509	0.86	-14,064	21,760
Weld Top	80601, 80609	4.14	41,628	48,004	601, 609	0.94	-14,779	28,012
	80701, 80709	4.42	43,987	66,924	701, 709	1.26	-13,354	69,191
	80801, 80809	4.69	44,617	61,564	801, 809	1.58	-7,519	74,168
	80901, 80909	4.97	43,308	67,306	901, 909	1.90	497	52,298
	81001, 81009	5.24	44,038	76,958	1001, 1009	2.22	10,202	25,356
	81101, 81009	5.51	38,226	60,103	1101, 1009	2.54	16,113	9,089
Weld Bottom	81201, 81209	5.79	22,896	53,576	1201, 1209	2.86	24,164	-1,327
	81301, 81309	6.03	13,248	831	1301, 1309	3.11	33,721	29,567
	81401, 81409	6.22	8,496	-18,301	1401, 1409	3.37	40,322	34,890
	81501, 81509	6.46	2,652	-19,265	1501, 1509	3.69	42,995	21,975
	81601, 81609	6.75	722	-6,024	1601, 1609	4.08	40,637	7,484
	81701, 81709	7.12	3,035	-398	1701, 1709	4.54	30,928	-1,532
	81801, 81809	7.58	3,482	93	1801, 1809	5.10	13,118	-1,793
	81901, 81909	8.16	3,272	385	1901, 1909	5.78	-1,786	-886
	82001, 82009	8.88	3,026	138	2001, 2009	6.60	1,598	557
	82101, 82109	9.78	3,136	-1,071	2101, 2109	7.58	3,956	714
	82201, 82209	10.90	3,506	-1,616	2201, 2209	8.77	2,989	327
	82301, 82309	12.31	3,537	-2,482	2301, 2309	10.21	2,902	205
	82401, 82409	13.07	3,037	827	2401, 2409	12.02	3,210	235
	Nozzle Bottom	82501, 82509	13.83	2,551	168	2501, 2509	13.83	2,625

Table 5-3d

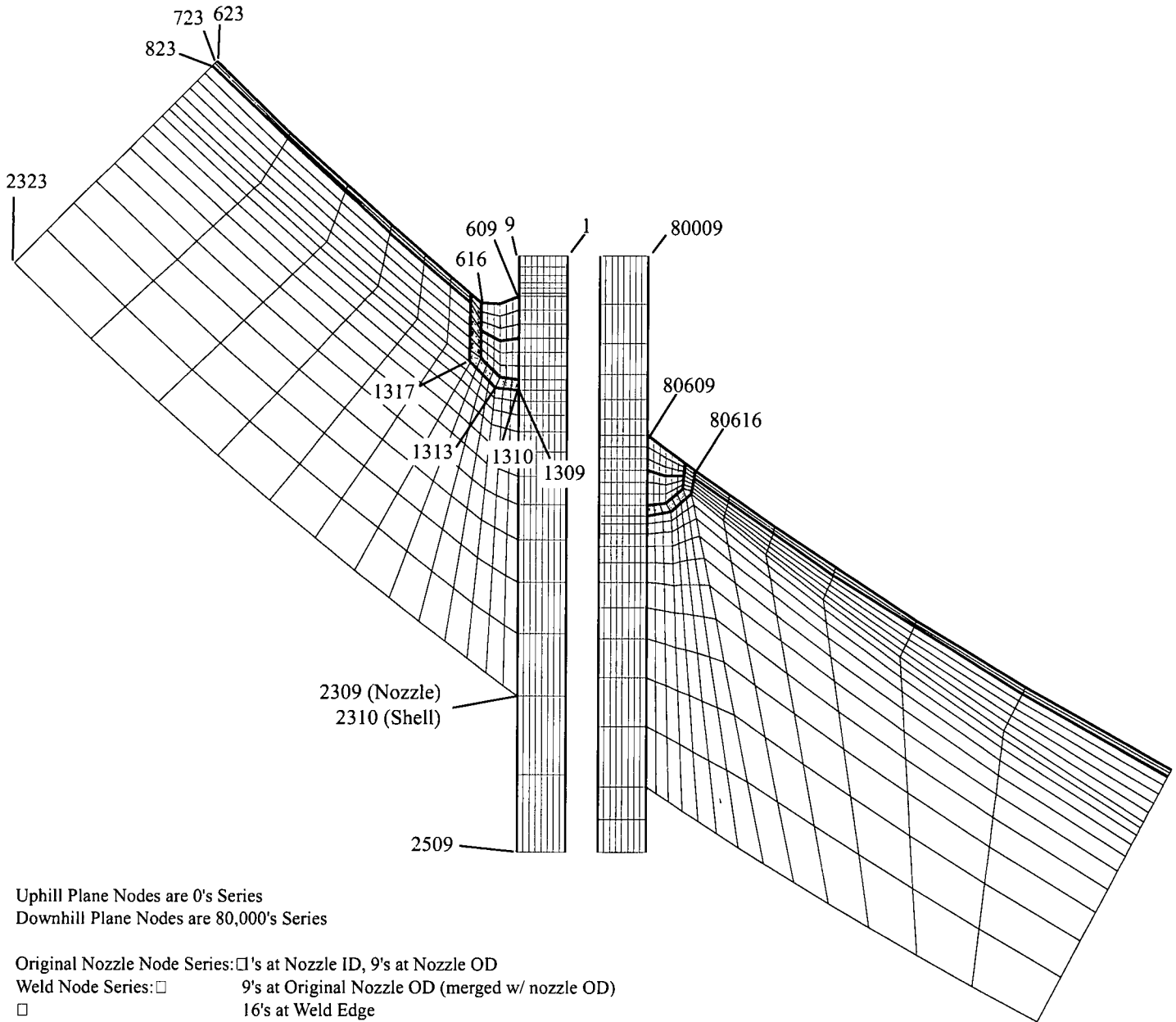
Nozzle ID and OD Hoop Stress (49.0° BMI Nozzle Case)

	Downhill Side			Uphill Side				
	Nodes	Axial Height	ID Hoop Stress (psi)	OD Hoop Stress (psi)	Nodes	Axial Height	ID Hoop Stress (psi)	OD Hoop Stress (psi)
Nozzle Top	80001, 80009	0.00	-3,722	-1,868	1, 9	0.00	621	-5,289
	80101, 80109	1.40	-6,680	-2,104	101, 109	0.21	-4,271	-10,584
	80201, 80209	2.53	9,655	-2,346	201, 209	0.38	-5,211	-15,056
	80301, 80309	3.43	39,134	3,915	301, 309	0.52	-7,466	-8,573
	80401, 80409	4.15	48,236	17,281	401, 409	0.63	-10,584	1,437
	80501, 80509	4.72	52,035	33,717	501, 509	0.72	-12,967	17,428
Weld Top	80601, 80609	5.19	54,862	37,236	601, 609	0.79	-14,636	17,751
	80701, 80709	5.51	55,735	60,921	701, 709	1.13	-14,658	66,848
	80801, 80809	5.83	50,873	55,490	801, 809	1.47	-12,418	71,984
	80901, 80909	6.16	46,672	61,176	901, 909	1.81	-5,445	48,644
	81001, 81009	6.48	38,565	69,994	1001, 1009	2.15	7,670	21,440
	81101, 81009	6.80	24,141	62,170	1101, 1009	2.49	21,677	2,532
Weld Bottom	81201, 81209	7.13	13,099	46,778	1201, 1209	2.83	29,289	-846
	81301, 81309	7.37	6,658	-12,381	1301, 1309	3.09	37,203	17,684
	81401, 81409	7.58	3,968	-30,370	1401, 1409	3.41	44,282	12,297
	81501, 81509	7.84	1,277	-21,886	1501, 1509	3.79	47,413	13,649
	81601, 81609	8.18	2,934	-4,790	1601, 1609	4.26	45,514	8,968
	81701, 81709	8.60	4,072	-778	1701, 1709	4.82	38,280	-4,341
	81801, 81809	9.12	3,860	176	1801, 1809	5.50	23,009	-5,588
	81901, 81909	9.79	3,187	338	1901, 1909	6.32	-1,728	-1,774
	82001, 82009	10.63	2,641	296	2001, 2009	7.31	-1,986	846
	82101, 82109	11.69	2,439	279	2101, 2109	8.51	4,724	969
	82201, 82209	13.02	2,588	311	2201, 2209	9.97	3,264	282
	82301, 82309	14.70	2,804	-686	2301, 2309	11.72	2,223	251
	82401, 82409	15.47	2,731	468	2401, 2409	13.98	2,705	275
Nozzle Bottom	82501, 82509	16.24	2,514	265	2501, 2509	16.24	2,588	227

Table 5-4

Change in Inner Diameter at Selected Axial Locations

Circ Location	Location 2 0.5" Above Uphill Weld Top		Location 3 Uphill Weld Top		Location 4 Uphill Weld Bottom		Location "X" Downhill Weld Top		
	Radial Deflection (mils)	Change in Diameter (mils)	Radial Deflection (mils)	Change in Diameter (mils)	Radial Deflection (mils)	Change in Diameter (mils)	Radial Deflection (mils)	Change in Diameter (mils)	
	Uphill	-90.0	0.47	0.94	0.17	0.34	0.85	1.70	0.17
0.0° Nozzle	-67.5	0.47	0.94	0.17	0.34	0.85	1.70	0.17	0.34
	-45.0	0.47	0.94	0.17	0.34	0.85	1.70	0.17	0.34
	-22.5	0.47	0.94	0.17	0.34	0.85	1.70	0.17	0.34
	0.0	0.47	0.94	0.17	0.34	0.85	1.70	0.17	0.34
	22.5	0.47	0.94	0.17	0.34	0.85	1.70	0.17	0.34
	45.0	0.47	0.94	0.17	0.34	0.85	1.70	0.17	0.34
	67.5	0.47	0.94	0.17	0.34	0.85	1.70	0.17	0.34
Downhill	90.0	0.47	0.94	0.17	0.34	0.85	1.70	0.17	0.34
Uphill	-90.0	23.10	0.16	19.75	-0.01	5.60	-0.34	3.97	-0.24
26.6° Nozzle	-67.5	21.35	0.16	18.31	0.08	5.41	0.09	3.99	0.31
	-45.0	16.37	0.17	14.13	0.25	4.84	1.25	3.82	1.61
	-22.5	8.90	0.17	7.80	0.41	3.52	2.36	3.15	2.95
	0.0	0.08	0.16	0.23	0.46	1.41	2.82	1.75	3.50
	22.5	-8.73	0.17	-7.39	0.41	-1.16	2.36	-0.20	2.95
	45.0	-16.20	0.17	-13.88	0.25	-3.59	1.25	-2.21	1.61
	67.5	-21.19	0.16	-18.23	0.08	-5.32	0.09	-3.68	0.31
Downhill	90.0	-22.94	0.16	-19.76	-0.01	-5.94	-0.34	-4.21	-0.24
Uphill	-90.0	32.09	0.09	28.08	-0.18	9.18	-3.40	0.50	-0.05
37.9° Nozzle	-67.5	29.65	0.09	25.99	-0.11	8.79	-2.61	0.59	0.38
	-45.0	22.70	0.07	19.98	0.03	7.53	-0.73	0.85	1.63
	-22.5	12.29	0.04	10.90	0.17	4.99	1.29	1.40	2.99
	0.0	0.02	0.04	0.11	0.22	1.06	2.12	1.82	3.64
	22.5	-12.25	0.04	-10.73	0.17	-3.70	1.29	1.59	2.99
	45.0	-22.63	0.07	-19.95	0.03	-8.26	-0.73	0.78	1.63
	67.5	-29.56	0.09	-26.10	-0.11	-11.40	-2.61	-0.21	0.38
Downhill	90.0	-32.00	0.09	-28.26	-0.18	-12.58	-3.40	-0.55	-0.05
Uphill	-90.0	39.29	0.20	34.97	-0.14	13.58	-4.82	-0.50	0.55
49.0° Nozzle	-67.5	36.29	0.16	32.34	-0.10	12.92	-3.92	-0.46	0.79
	-45.0	27.75	0.07	24.80	-0.03	10.87	-1.60	-0.20	1.51
	-22.5	15.00	-0.01	13.46	0.03	6.93	0.90	0.33	2.15
	0.0	-0.03	-0.06	0.02	0.04	0.97	1.94	1.20	2.40
	22.5	-15.01	-0.01	-13.43	0.03	-6.03	0.90	1.82	2.15
	45.0	-27.68	0.07	-24.83	-0.03	-12.47	-1.60	1.71	1.51
	67.5	-36.13	0.16	-32.44	-0.10	-16.84	-3.92	1.25	0.79
Downhill	90.0	-39.09	0.20	-35.11	-0.14	-18.40	-4.82	1.05	0.55



Uphill Plane Nodes are 0's Series
 Downhill Plane Nodes are 80,000's Series

Original Nozzle Node Series: □'s at Nozzle ID, 9's at Nozzle OD
 Weld Node Series: □ 9's at Original Nozzle OD (merged w/ nozzle OD)
 □ 16's at Weld Edge
 Shell Node Series: □ 10's at Penetration ID below weld region
 □ 23's at edge of shell section

Node Numbers Increase by 100 up the length of the tube and shell
 Node Numbers Increase by 1 along the tube and shell radius

Bottom Head Instrumentation Nozzle Node Numbering Scheme

Figure 5-1

Enclosure - Attachment 2

C-7789-00-2

Revision 1

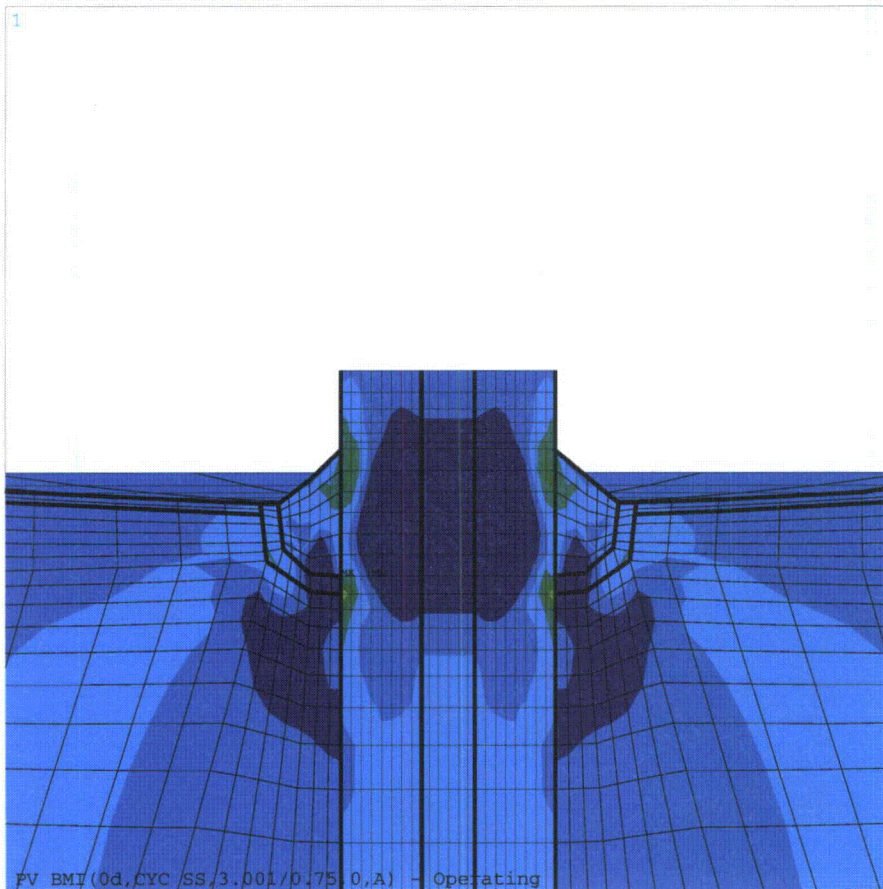
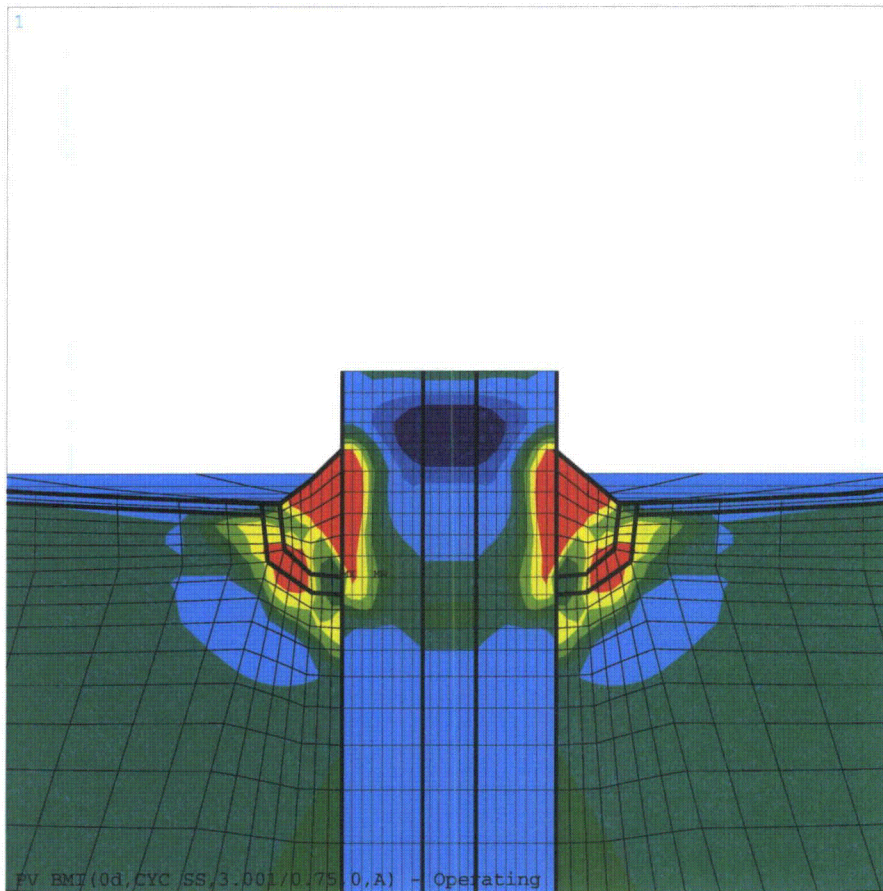
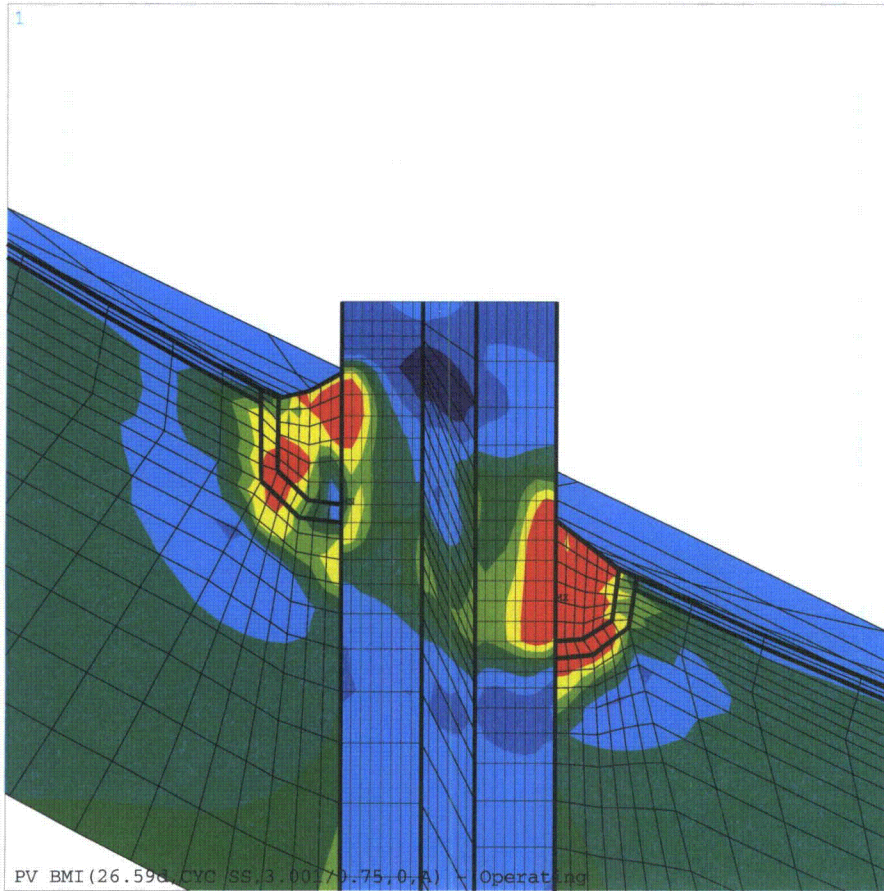


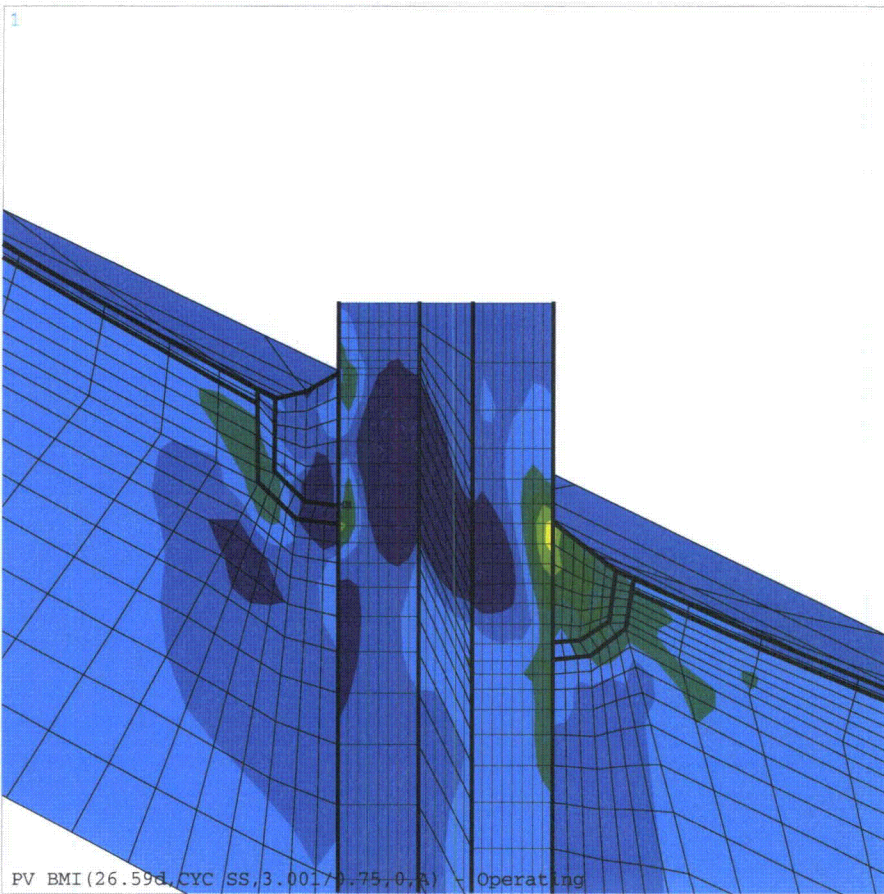
Figure 5-2

Operating plus Residual
Hoop (SY) and Axial (SZ) Stress
0.0° BMI Nozzle



ANSYS 8.0
JUL 23 2004
16:06:33
PLOT NO. 2
NODAL SOLUTION
TIME=7004
SZ (AVG)
RSYS=11
PowerGraphics
EFACET=1
AVRES=All
DMX =.443919
SMN =-82736
SMX =85580

Dark Blue	-82736
Blue	-10000
Light Blue	0
Green	10000
Dark Green	20000
Yellow-Green	30000
Yellow	40000
Orange	50000
Red	100000

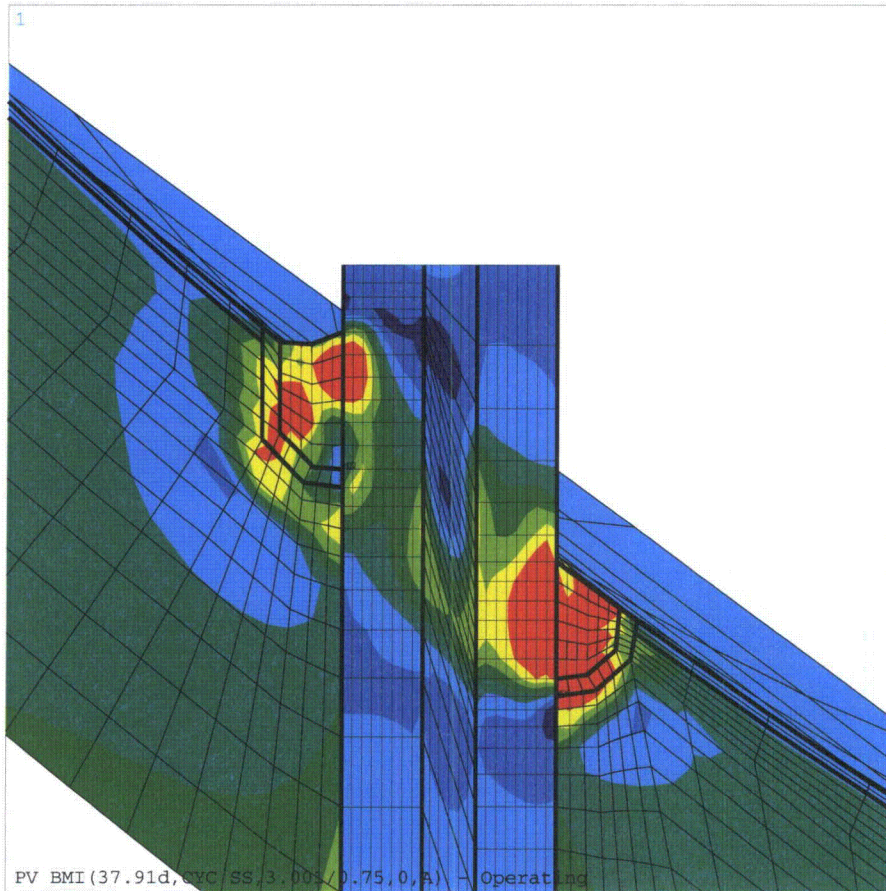


ANSYS 8.0
JUL 23 2004
16:06:33
PLOT NO. 2
NODAL SOLUTION
TIME=7004
SZ (AVG)
RSYS=11
PowerGraphics
EFACET=1
AVRES=All
DMX =.443919
SMN =-82736
SMX =85580

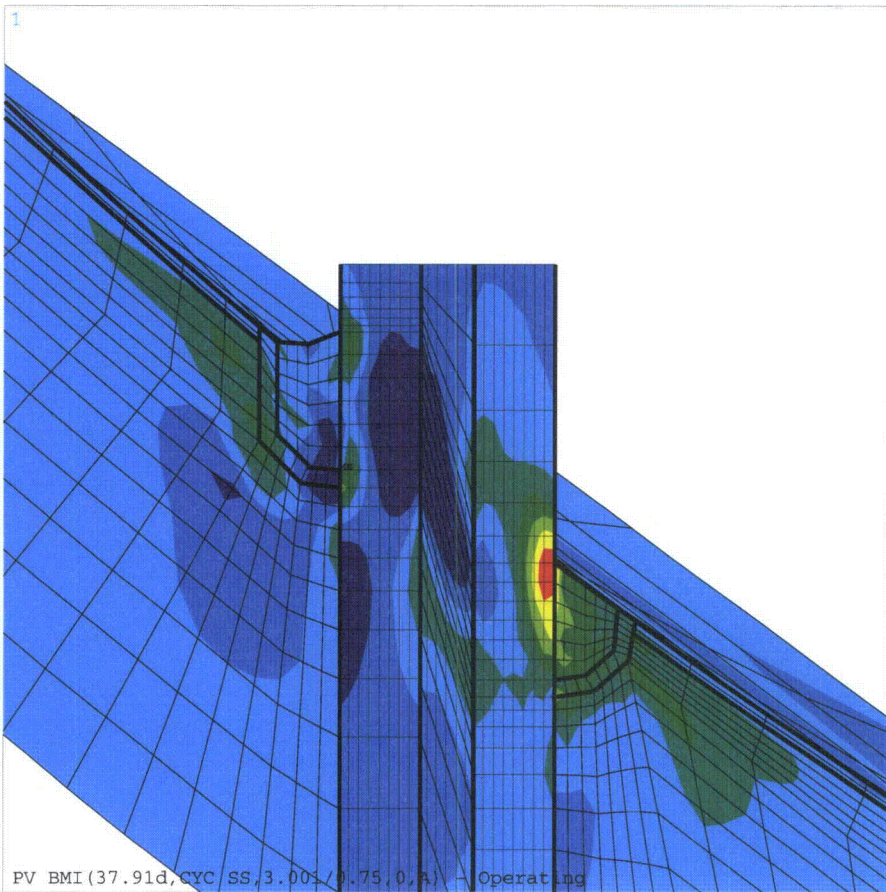
Dark Blue	-82736
Blue	-10000
Light Blue	0
Green	10000
Dark Green	20000
Yellow-Green	30000
Yellow	40000
Orange	50000
Red	100000

Figure 5-3

Operating plus Residual
Hoop (SY) and Axial (SZ) Stress
26.6° BMI Nozzle



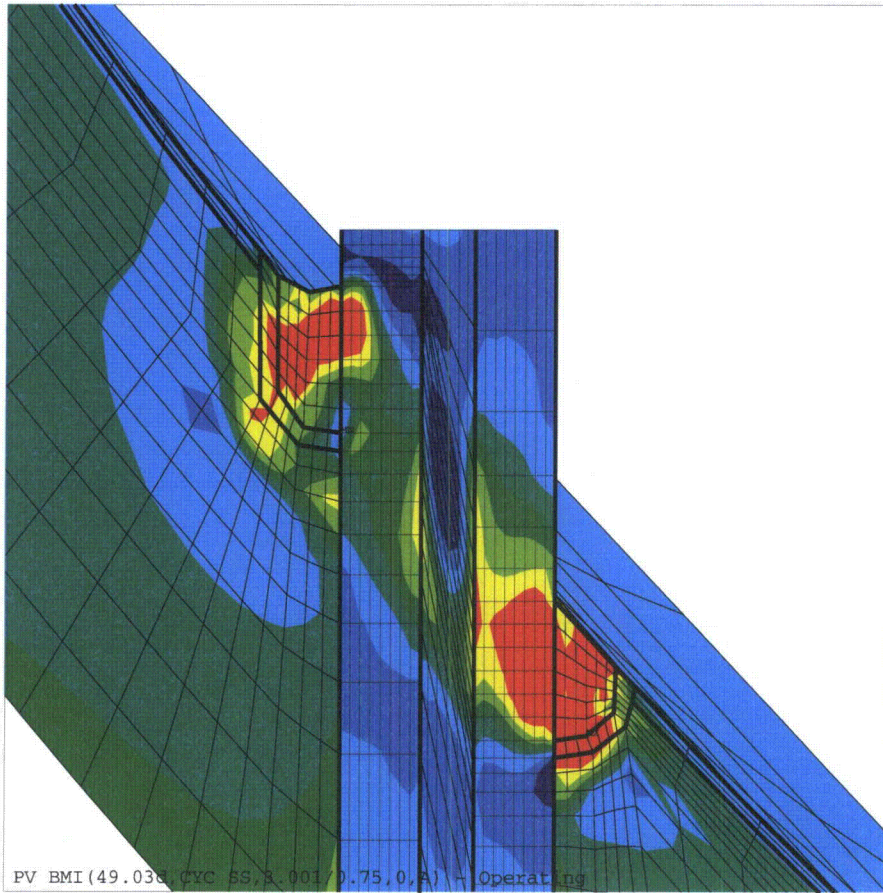
ANSYS 8.0
JUL 23 2004
16:06:42
PLOT NO. 1
NODAL SOLUTION
TIME=7004
SY (AVG)
RSYS=11
PowerGraphics
EFACET=1
AVRES=All
DMX =.440476
SMN =-70462
SMX =80177
-70462
-10000
0
10000
20000
30000
40000
50000
100000



ANSYS 8.0
JUL 23 2004
16:06:43
PLOT NO. 2
NODAL SOLUTION
TIME=7004
SZ (AVG)
RSYS=11
PowerGraphics
EFACET=1
AVRES=All
DMX =.440476
SMN =-81501
SMX =89427
-81501
-10000
0
10000
20000
30000
40000
50000
100000

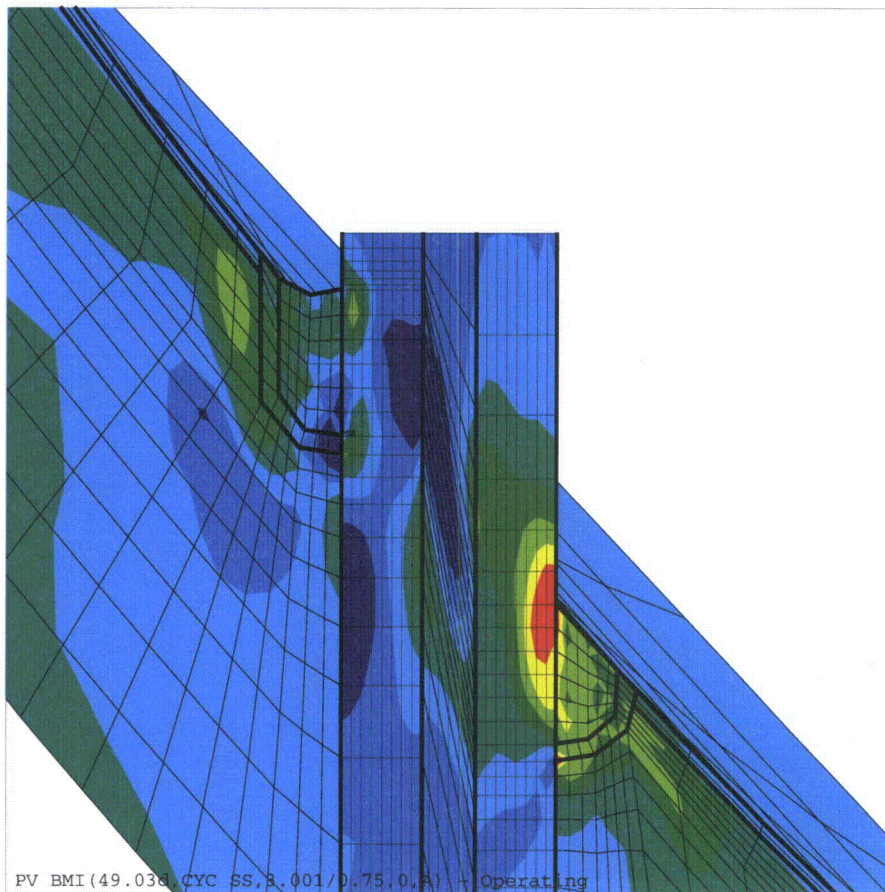
Figure 5-4

Operating plus Residual
Hoop (SY) and Axial (SZ) Stress
37.9° BMI Nozzle



ANSYS 8.0
 JUL 23 2004
 16:06:53
 PLOT NO. 1
 NODAL SOLUTION
 TIME=7004
 SY (AVG)
 RSYS=11
 PowerGraphics
 EFACET=1
 AVRES=All
 DMX =.444361
 SMN =-60928
 SMX =81967

Dark Blue	-60928
Blue	-10000
Light Blue	0
Green	10000
Dark Green	20000
Yellow-Green	30000
Yellow	40000
Orange	50000
Red	100000

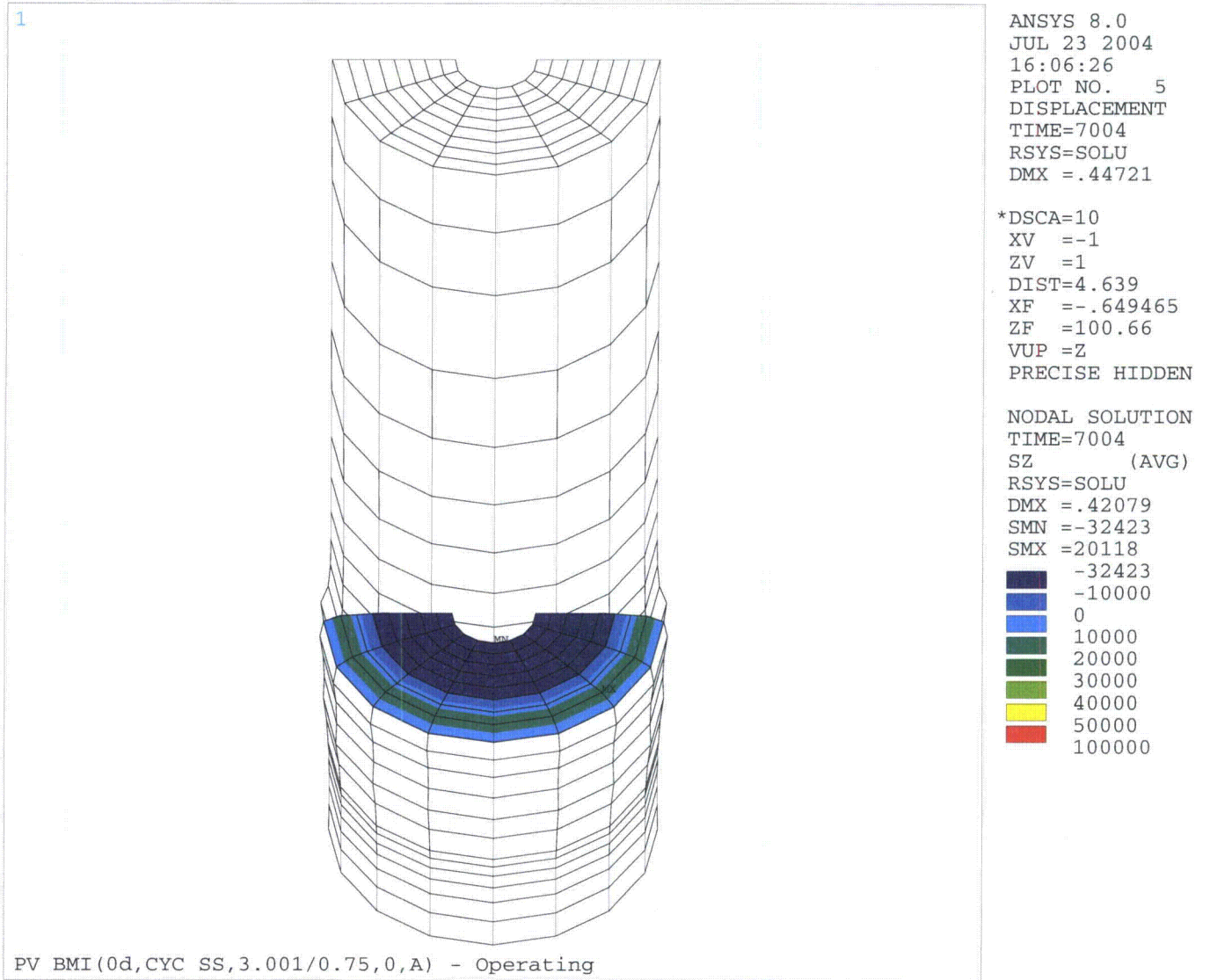


ANSYS 8.0
 JUL 23 2004
 16:06:54
 PLOT NO. 2
 NODAL SOLUTION
 TIME=7004
 SZ (AVG)
 RSYS=11
 PowerGraphics
 EFACET=1
 AVRES=All
 DMX =.444361
 SMN =-80944
 SMX =88533

Dark Blue	-80944
Blue	-10000
Light Blue	0
Green	10000
Dark Green	20000
Yellow-Green	30000
Yellow	40000
Orange	50000
Red	100000

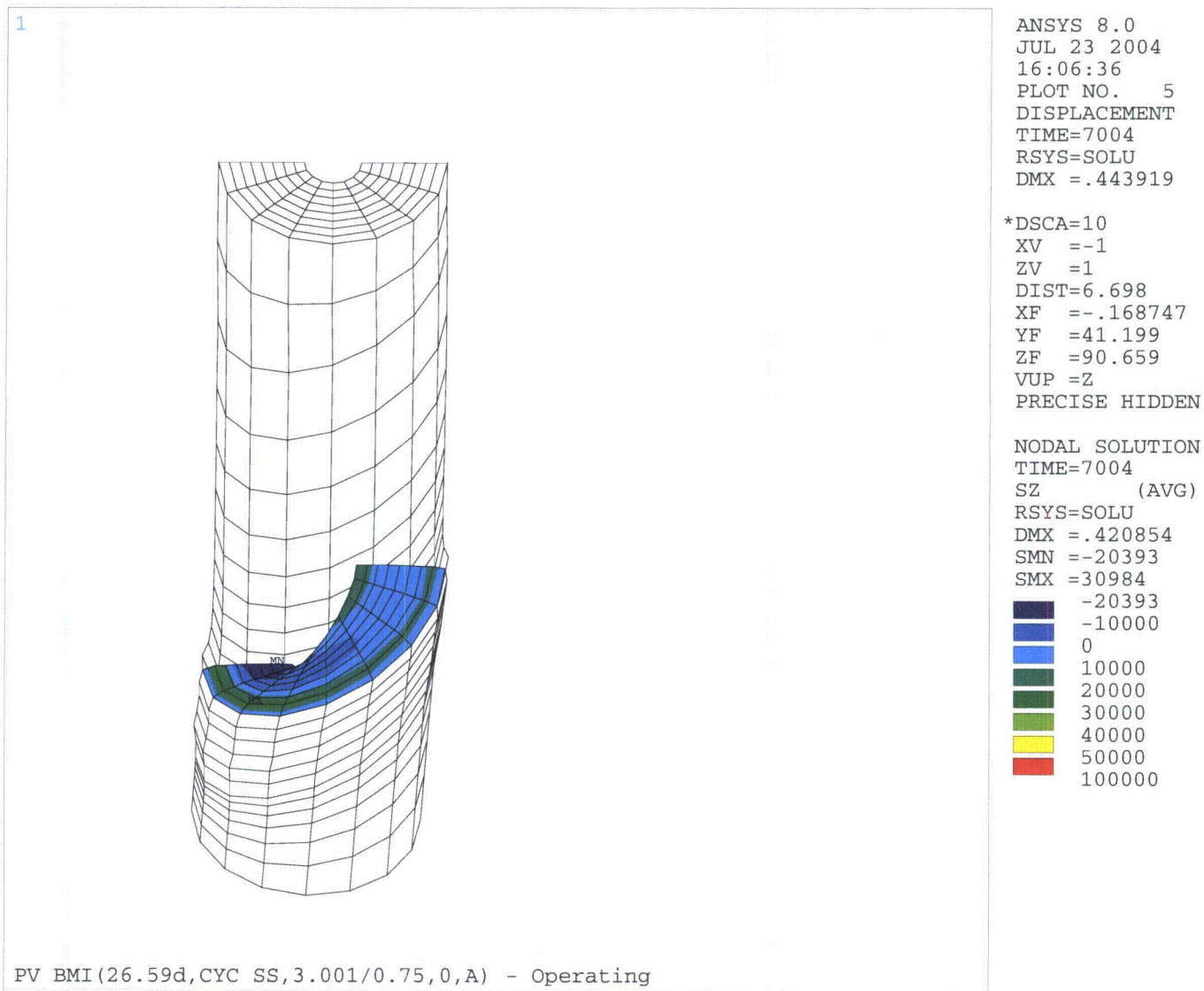
Figure 5-5

Operating plus Residual
 Hoop (SY) and Axial (SZ) Stress
 49.0° BMI Nozzle



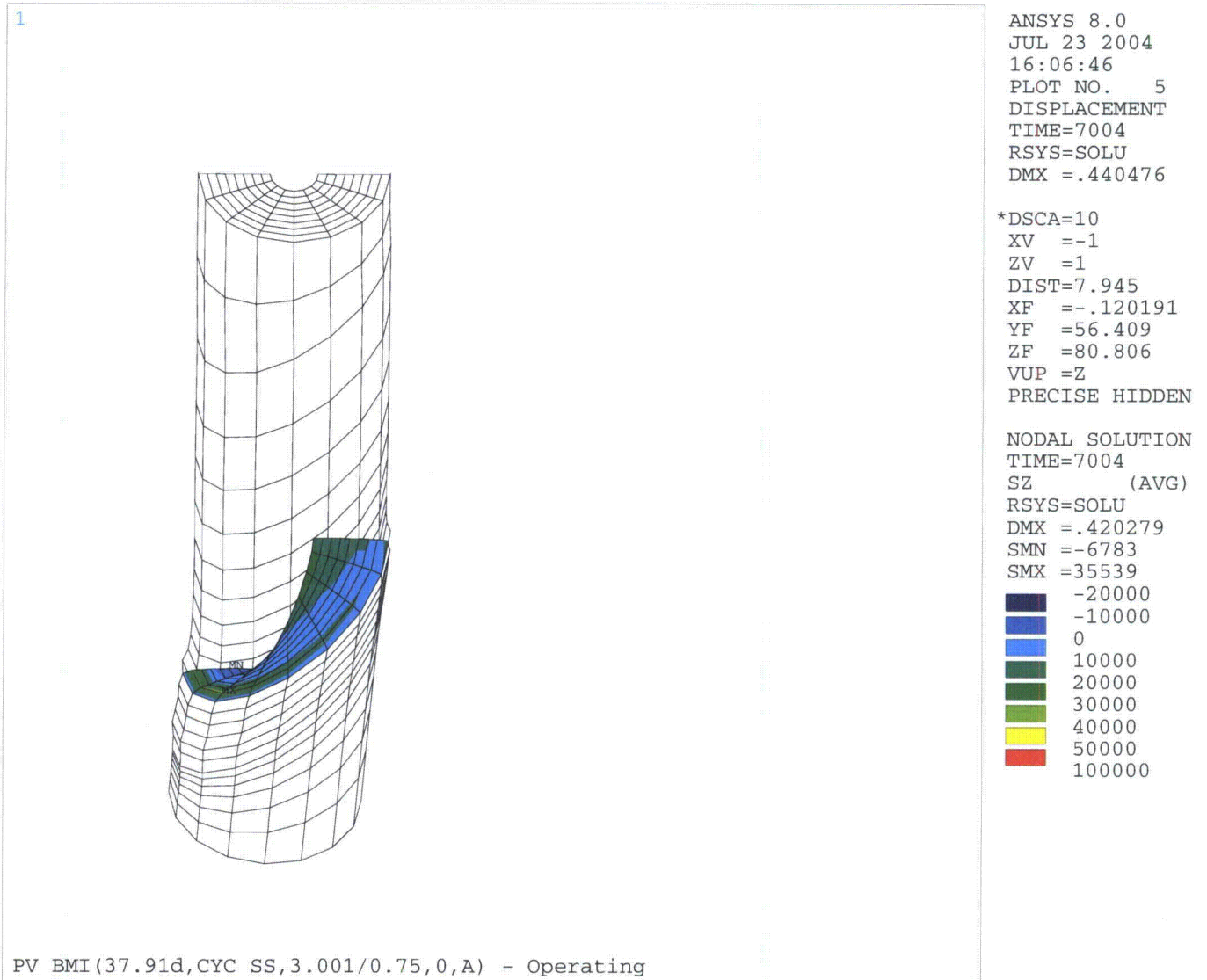
Operating Plus Residual Axial Stress at Bottom of Weld - Element-Oriented
Coordinate System - 0.0° BMI

Figure 5-6



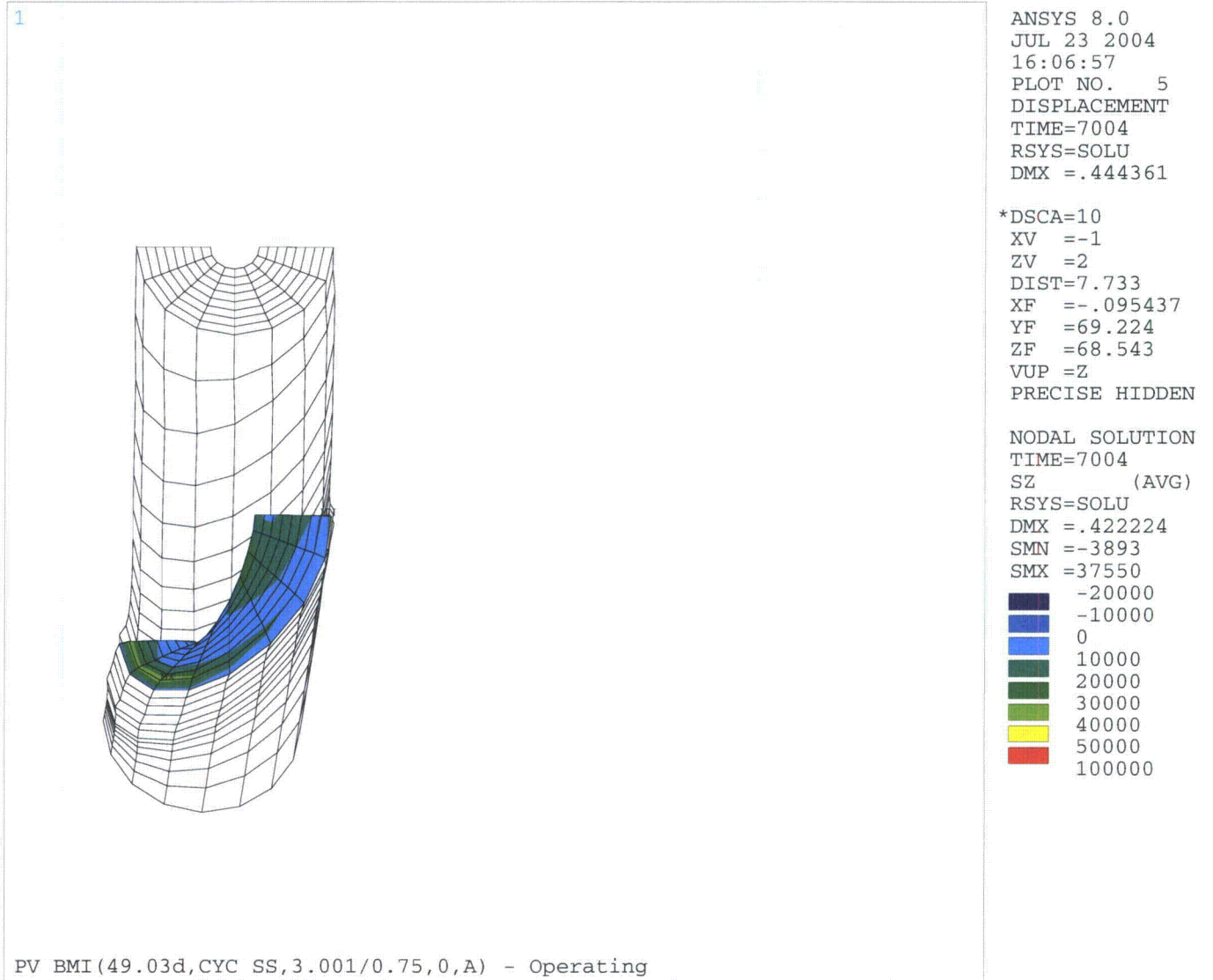
Operating Plus Residual Axial Stress at Bottom of Weld - Element-Oriented
Coordinate System - 26.6° BMI

Figure 5-7



Operating Plus Residual Axial Stress at Bottom of Weld - Element-Oriented
Coordinate System - 37.9° BMI

Figure 5-8



Operating Plus Residual Axial Stress at Bottom of Weld - Element-Oriented
Coordinate System - 49.0° BMI

Figure 5-9

Enclosure - Attachment 2

Document No.: C-7789-00-2

Revision No.: 1

Attachment Page: 1 of 4

DESCRIPTION: FEA of Palo Verde BMI NOZZLES (0.0 DEG)
 REVISION A: Westinghouse Cyclic Stress-Strain Nozzle Props

ANALYSIS DATE (YYMMDD): 20040524. ANSYS VERSION: 8.0
 cirse.base MODEL VERSION: 2.4.6
 TITLE: PV BMI (0.0d, 45.2k, 3.00/0.75, 0.000,A)

	Max. Hoop Stress (psi)		Max. Axial Stress (psi)	
	Downhill	Uphill	Downhill	Uphill
I.S. Below Weld	21851.	21851.	817.	817.
I.S. Above Weld	16457.	16457.	-576.	-576.
Midwall Below Weld	27495.	27495.		
Midwall Above Weld	12575.	12575.		

Max. Lateral Deflection: -.0000" Max. Ovality: 0.0000"

***** INSIDE SURFACE STRESSES (psi) *****

```

** Uphill side, above weld **
Max Hoop @ Node 1. Hoop : 16457. Axial: -576. Ratio:-28.55
Max Axial @ Node 1. Axial: -576. Hoop : 16457. Ratio:-28.55
** Uphill side, below weld **
Max Hoop @ Node 1401. Hoop : 21851. Axial: -11924. Ratio: -1.83
Max Axial @ Node 1901. Axial: 817. Hoop : 3118. Ratio: 3.82
** Downhill side, above weld **
Max Hoop @ Node 80001. Hoop : 16457. Axial: -576. Ratio:-28.55
Max Axial @ Node 80001. Axial: -576. Hoop : 16457. Ratio:-28.55
** Downhill side, below weld **
Max Hoop @ Node 81401. Hoop : 21851. Axial: -11924. Ratio: -1.83
Max Axial @ Node 81901. Axial: 817. Hoop : 3118. Ratio: 3.82
    
```

***** INPUT PARAMETERS *****

```

SYD=45172. HDALLOY=533. HPRESS=3110. OPRESS=2250.
CTHK=0.1600 STHK=6.6600 SA=96.5200 THETA= 0.00 TOR=1.5005
TIR=0.3750 HCBOR=0.000 HCBOTZ= 0.000 LTIP=1.9000
HGRATE= 75. TRIMFLAG=0. OTEMP=565. BUTTFIX=2.
BOTZAUTO=0. HCBOTINC= 0.000 PARATRIM=0. TRIMANG= 0.00
FOURPASS=0. PRESSFLG=0.
CYLSHELL=0. NOBUTTER=0. STRRLF=1.

DD1= 1.0000 DD2= 1.2500 DD3= 0.6325 DD4= 0.8145 DD5= 0.8094
DD6= 1.0397 DD7= 0.8795 DD8= 1.1295 DD9= 1.1119 DD10= 0.4397
DD11=-0.3450 DDRF= 0.7824

UU1= 1.0000 UU2= 1.2500 UU3= 0.6325 UU4= 0.8145 UU5= 0.8094
UU6= 1.0397 UU7= 0.8795 UU8= 1.1295 UU9= 1.1119 UU10= 0.4397
UU11=-0.3450 UURF= 0.7824

NCIRC= 8. CIRC_EXT=180. NRTUBE= 8. NRWELD= 6. NRBUTT= 1.
NRBASE= 6. NATTIP= 6. NACLAD= 2. NAWELD= 6. NAHOLE=10.
NAEXTN= 2. GRAD1= 6.0 GRAD2= 4.0 GRAD3= 4.0 GRAD4= 5.0
GRAD5= 5.5 GRAD6= 7.9 GSTIF=0.50E+09

F_REP= 0. W_REP= 0.

EMB_FLAW= 0.

Head Counterbore Unselect Flags (0-8 in order): 0. 0. 0. 0. 0. 0. 0. 0. 0.
Tube Counterbore Unselect Flags (0-8 in order): 0. 0. 0. 0. 0. 0. 0. 0. 0.

HGTARG=3350.0 PASS1MXT=3337.2 PASS2MXT=3362.6
    
```

Enclosure - Attachment 2

Document No.: C-7789-00-2

Revision No.: 1

Attachment Page: 2 of 4

DESCRIPTION: FEA of Palo Verde BMI NOZZLES (26.59 DEG)
REVISION A: Westinghouse Cyclic Stress-Strain Nozzle Props

ANALYSIS DATE (YYMMDD): 20040524. ANSYS VERSION: 8.0
cirse.base MODEL VERSION: 2.4.6
TITLE: PV BMI (26.6d, 45.2k, 3.00/0.75, 0.000,A)

Table with 5 columns: Location, Max. Hoop Stress (psi) Downhill, Max. Hoop Stress (psi) Uphill, Max. Axial Stress (psi) Downhill, Max. Axial Stress (psi) Uphill. Rows include I.S. Below Weld, I.S. Above Weld, Midwall Below Weld, Midwall Above Weld.

Max. Lateral Deflection: 0.0261" Max. Ovality: 0.0039"

***** INSIDE SURFACE STRESSES (psi) *****

** Uphill side, above weld **
Max Hoop @ Node 1. Hoop : 3125. Axial: -3457. Ratio: -0.90
Max Axial @ Node 1. Axial: -3457. Hoop : 3125. Ratio: -0.90
** Uphill side, below weld **
Max Hoop @ Node 1501. Hoop : 35655. Axial: 2908. Ratio: 12.26
Max Axial @ Node 1601. Axial: 8477. Hoop : 31781. Ratio: 3.75
** Downhill side, above weld **
Max Hoop @ Node 80501. Hoop : 34552. Axial: -9428. Ratio: -3.66
Max Axial @ Node 80101. Axial: -931. Hoop : -2672. Ratio: 2.87
** Downhill side, below weld **
Max Hoop @ Node 81101. Hoop : 38921. Axial: 572. Ratio: 68.04
Max Axial @ Node 81401. Axial: 10586. Hoop : 13336. Ratio: 1.26

***** INPUT PARAMETERS *****

SYD=45172. HDALLOY=533. HPRESS=3110. OPRESS=2250.
CTHK=0.1600 STHK=6.6600 SA=96.5200 THETA=26.59 TOR=1.5005
TIR=0.3750 HCBOR=0.000 HCBOTZ= 0.000 LTIP=2.6000
HGRATE= 75. TRIMFLAG=0. OTEMP=565. BUTTFIX=2.
BOTZAUTO=0. HCBOTINC= 0.000 PARATRIM=0. TRIMANG= 0.00
FOURPASS=0. PRESSFLG=0.
CYLSHELL=0. NOBUTTER=0. STRRLF=1.

DD1= 0.9080 DD2= 1.1315 DD3= 0.8996 DD4= 1.1317 DD5= 0.8905
DD6= 1.1150 DD7= 0.8795 DD8= 1.1295 DD9= 1.1295 DD10= 0.4398
DD11=-0.3016 DDRF= 0.7338

UU1= 1.2739 UU2= 1.4975 UU3= 0.6803 UU4= 0.6694 UU5= 0.7894
UU6= 1.0194 UU7= 0.8795 UU8= 1.1295 UU9= 1.1032 UU10= 0.4398
UU11=-0.1187 UURF= 0.2373

NCIRC= 8. CIRC_EXT=180. NRTUBE= 8. NRWELD= 6. NR BUTT= 1.
NRBASE= 6. NATTIP= 6. NA CLAD= 2. NAWELD= 6. NAHOLE=10.
NAEXTN= 2. GRAD1= 6.0 GRAD2= 4.0 GRAD3= 4.0 GRAD4= 5.0
GRAD5= 5.5 GRAD6= 7.9 GSTIF=0.50E+09

F_REP= 0. W_REP= 0.

EMB_FLAW= 0.

Head Counterbore Unselect Flags (0-8 in order): 0. 0. 0. 0. 0. 0. 0. 0. 0.
Tube Counterbore Unselect Flags (0-8 in order): 0. 0. 0. 0. 0. 0. 0. 0. 0.

HGTARG=3350.0 PASS1MXT=3347.7 PASS2MXT=3354.0

Enclosure - Attachment 2

Document No.: C-7789-00-2

Revision No.: 1

Attachment Page: 3 of 4

DESCRIPTION: FEA of Palo Verde BMI NOZZLES (37.91 DEG)
REVISION A: Westinghouse Cyclic Stress-Strain Nozzle Props

ANALYSIS DATE (YYMMDD): 20040524. ANSYS VERSION: 8.0
cirse.base MODEL VERSION: 2.4.6
TITLE: PV BMI (37.9d, 45.2k, 3.00/0.75, 0.000,A)

	Max. Hoop Stress (psi)		Max. Axial Stress (psi)	
	Downhill	Uphill	Downhill	Uphill
I.S. Below Weld	44617.	42995.	16799.	20096.
I.S. Above Weld	43700.	651.	19201.	-2706.
Midwall Below Weld	55978.	27288.		
Midwall Above Weld	41823.	0.		

Max. Lateral Deflection: 0.0354" Max. Ovality: 0.0073"

***** INSIDE SURFACE STRESSES (psi) *****

```

** Uphill side, above weld **
Max Hoop @ Node 1. Hoop : 651. Axial: -3471. Ratio: -0.19
Max Axial @ Node 501. Axial: -2706. Hoop : -14064. Ratio: 5.20
** Uphill side, below weld **
Max Hoop @ Node 1501. Hoop : 42995. Axial: 14196. Ratio: 3.03
Max Axial @ Node 1601. Axial: 20096. Hoop : 40637. Ratio: 2.02
** Downhill side, above weld **
Max Hoop @ Node 80501. Hoop : 43700. Axial: 7472. Ratio: 5.85
Max Axial @ Node 80401. Axial: 19201. Hoop : 43165. Ratio: 2.25
** Downhill side, below weld **
Max Hoop @ Node 80801. Hoop : 44617. Axial: -1712. Ratio:-26.06
Max Axial @ Node 81101. Axial: 16799. Hoop : 38226. Ratio: 2.28

```

***** INPUT PARAMETERS *****

```

SYD=45172. HDALLOY=533. HPRESS=3110. OPRESS=2250.
CTHK=0.1600 STHK=6.6600 SA=96.5200 THETA=37.91 TOR=1.5005
TIR=0.3750 HCBOR=0.000 HCBOTZ= 0.000 LTIP=3.0000
HGRATE= 75. TRIMFLAG=0. OTEMP=565. BUTTFIX=2.
BOTZAUTO=0. HCBOTINC= 0.000 PARATRIM=0. TRIMANG= 0.00
FOURPASS=0. PRESSFLG=0.
CYLSHELL=0. NOBUTTER=0. STRRLF=1.

```

```

DD1= 0.8167 DD2= 1.0139 DD3= 0.9825 DD4= 1.2118 DD5= 0.8795
DD6= 1.1295 DD7= 0.8795 DD8= 1.1295 DD9= 1.1295 DD10= 0.4397
DD11=-0.2584 DDRF= 0.6718

```

```

UU1= 1.3215 UU2= 1.5187 UU3= 0.5118 UU4= 0.5006 UU5= 0.8277
UU6= 1.0325 UU7= 0.8795 UU8= 1.1284 UU9= 1.0978 UU10= 0.4397
UU11=-0.0000 UURF= 0.0000

```

```

NCIRC= 8. CIRC_EXT=180. NRTUBE= 8. NRWELD= 6. NRBUTT= 1.
NRBASE= 6. NATTIP= 6. NACLAD= 2. NAWELD= 6. NAHOLE=10.
NAEXTN= 2. GRAD1= 6.0 GRAD2= 4.0 GRAD3= 4.0 GRAD4= 5.0
GRAD5= 5.5 GRAD6= 7.9 GSTIF=0.50E+09

```

F_REP= 0. W_REP= 0.

EMB_FLAW= 0.

Head Counterbore Unselect Flags (0-8 in order): 0. 0. 0. 0. 0. 0. 0. 0. 0. 0.
Tube Counterbore Unselect Flags (0-8 in order): 0. 0. 0. 0. 0. 0. 0. 0. 0. 0.

HGTARG=3350.0 PASS1MXT=3346.6 PASS2MXT=3355.3

Enclosure - Attachment 2

Document No.: C-7789-00-2

Revision No.: 1

Attachment Page: 4 of 4

DESCRIPTION: FEA of Palo Verde BMI NOZZLES (49.03 DEG)
REVISION A: Westinghouse Cyclic Stress-Strain Nozzle Props

ANALYSIS DATE (YYMMDD): 20040524. ANSYS VERSION: 8.0
cirse.base MODEL VERSION: 2.4.6
TITLE: PV BMI (49.0d, 45.2k, 3.00/0.75, 0.000,A)

Table with 5 columns: Location, Max. Hoop Stress (psi) Downhill, Max. Hoop Stress (psi) Uphill, Max. Axial Stress (psi) Downhill, Max. Axial Stress (psi) Uphill. Rows include I.S. Below Weld, I.S. Above Weld, Midwall Below Weld, Midwall Above Weld.

Max. Lateral Deflection: 0.0416" Max. Ovality: 0.0099"

***** INSIDE SURFACE STRESSES (psi) *****

** Uphill side, above weld **
Max Hoop @ Node 1. Hoop : 621. Axial: -3368. Ratio: -0.18
Max Axial @ Node 401. Axial: -1200. Hoop : -10584. Ratio: 8.82
** Uphill side, below weld **
Max Hoop @ Node 1501. Hoop : 47413. Axial: 24156. Ratio: 1.96
Max Axial @ Node 1601. Axial: 28412. Hoop : 45514. Ratio: 1.60
** Downhill side, above weld **
Max Hoop @ Node 80601. Hoop : 54862. Axial: 18023. Ratio: 3.04
Max Axial @ Node 80401. Axial: 32703. Hoop : 48236. Ratio: 1.48
** Downhill side, below weld **
Max Hoop @ Node 80701. Hoop : 55735. Axial: 18405. Ratio: 3.03
Max Axial @ Node 81001. Axial: 20399. Hoop : 38565. Ratio: 1.89

***** INPUT PARAMETERS *****

SYD=45172. HDALLOY=533. HPRESS=3110. OPRESS=2250.
CTHK=0.1600 STHK=6.6600 SA=96.5200 THETA=49.03 TOR=1.5005
TIR=0.3750 HCBOR=0.000 HCBOTZ= 0.000 LTIP=3.5000
HGRATE= 75. TRIMFLAG=0. OTEMP=565. BUTTFIX=2.
BOTZAUTO=0. HCBOTINC= 0.000 PARATRIM=0. TRIMANG= 0.00
FOURPASS=0. PRESSFLG=0.
CYLSHELL=0. NOBUTTER=0. STRRLF=1.

DD1= 0.7071 DD2= 0.8710 DD3= 1.0086 DD4= 1.2719 DD5= 0.8795
DD6= 1.1295 DD7= 0.8795 DD8= 1.1295 DD9= 1.1295 DD10= 0.4397
DD11=-0.2005 DDRF= 0.5947

UU1= 1.3189 UU2= 1.4828 UU3= 0.4519 UU4= 0.4687 UU5= 0.8288
UU6= 0.9909 UU7= 0.8795 UU8= 1.1288 UU9= 1.0817 UU10= 0.4397
UU11=-0.0000 UURF= 0.0000

NCIRC= 8. CIRC_EXT=180. NRTUBE= 8. NRWELD= 6. NRBUTT= 1.
NRBASE= 6. NATTIP= 6. NACLAD= 2. NAWELD= 6. NAHOLE=10.
NAEXTN= 2. GRAD1= 6.0 GRAD2= 4.0 GRAD3= 4.0 GRAD4= 5.0
GRAD5= 5.5 GRAD6= 7.9 GSTIF=0.50E+09

F_REP= 0. W_REP= 0.

EMB_FLAW= 0.

Head Counterbore Unselect Flags (0-8 in order): 0. 0. 0. 0. 0. 0. 0. 0. 0.
Tube Counterbore Unselect Flags (0-8 in order): 0. 0. 0. 0. 0. 0. 0. 0. 0.

HGTARG=3350.0 PASS1MXT=3341.9 PASS2MXT=3357.9

Enclosure - Attachment 2

Document No.: C-7789-00-2

Revision No.: 1

Attachment Page: 1 of 6

```

RESU,,dbs,.. /
/PAGE,,,10000,200
/POST1
file,,rst,.. /
!
TW4=1.5      ! zoom in for weld plots
!
/GRAPHICS,FULL
CSYS,11
CLOCAL,71,1,0,0,NZ(1+NRTUBE)      ! Local CSYS at lower tube edge
CSYS,11
RSYS,11
/COM,
/COM, -----
/COM, **** Get lateral deflection and ovality ****
/COM, -----
/COM,
SET,,,,,T0+1.0
*DO,I,0,ncirc,1
  *DIM,DEFCOL%I%,TABLE,(NNUM23-1)/100+1
*ENDDO
*DIM,LOC2DEF,ARRAY,ncirc+1      ! Location 2 is 0.5" below downhill weld
*DIM,LOC3DEF,ARRAY,ncirc+1      ! Location 3 is at the bottom of the downhill weld
*DIM,LOC4DEF,ARRAY,ncirc+1      ! Location 4 is at the top of the downhill weld
*DIM,LOCXDEF,ARRAY,ncirc+1      ! Location "X" is at the bottom of the uphill weld
RSYS,11
/COM,
/COM, ** Fill node axial distance vs. radial deflection table arrays
*DO,I,0,ncirc,1
  K=1
  *DO,J,I*10000+1,I*10000+NNUM23,100
    DEFCOL%I%(K)=UX(J)
    DEFCOL%I%(K,0)=NZ(J)
    K=K+1
  *ENDDO
*ENDDO
*DO,I,0,ncirc,1
  DEFCOL%I%(0,1)=1.0
*ENDDO
/COM,
/COM, ** Interpolate to get deflection and ovality at desired locations
*DO,I,0,ncirc,0
  LOC2DEF(I+1)=DEFCOL%I%(NZ(NNUM1)-0.5)
  LOC3DEF(I+1)=DEFCOL%I%(NZ(NNUM1))
  LOC4DEF(I+1)=DEFCOL%I%(NZ(NNUM14))
  LOCXDEF(I+1)=DEFCOL%I%(NZ(ncirc*10000+NNUM1))
*ENDDO
*GET,FNAME,ACTIVE,0,JOBNAM
/OUT,%FNAME%.W_Data,out
/COM,
/COM,          RADIAL DEF   RADIAL DEF   RADIAL DEF   RADIAL DEF
/COM,COL #      @ LOC 2      @ LOC 3      @ LOC 4      @ LOC "X"
*VWRITE,SEQU,LOC2DEF(1),LOC3DEF(1),LOC4DEF(1),LOCXDEF(1)
(F5.0,3X,5(F10.5,3X))
/COM,
/COM, -----
/COM, *****
/COM, -----
/COM,
/OUT
/COM,
/COM, -----
/COM,          **** Get gap force data ****

```

Enclosure - Attachment 2

Document No.: C-7789-00-2

Revision No.: 1

Attachment Page: 2 of 6

```
/COM, -----
/COM,
!
SET,,,,,T0+4.0
!
ETABLE,GAPFORCE,SMISC,2
ESEL,S,TYPE,,2
ESEL,R,REAL,,1
/OUT,%FNAME%.W_Data,out,,APPEND
/COM, Force in all gap elements in interference region
PRETAB
/COM,
/COM,
/OUT,
NSLE
NSEL,R,NODE,,1+NRTUBE,(ncirc+1)*10000,100
NSEL,A,NODE,,1+NRTUBE
DSYS,71
/OUT,%FNAME%.W_Data,out,,APPEND
/COM, Location of all gap elements in interference region - Rel to tube bottom OD
NLIST
/COM,
/COM, -----
/COM,
/OUT,
/COM,
/COM, -----
/COM,          **** Get stress data ****
/COM, -----
/COM,
NSEL,ALL
ESEL,ALL
NTMP1=NODE(NX(1),NY(1),NZ(NNUM1)-0.5)          ! Node 0.5" below downhill weld
NTMP2=NODE(NX(ncirc*10000+1),NY(ncirc*10000+1),NZ(ncirc*10000+NNUM1)-0.5)      ! Node 0.5"
below uphill weld
NSEL,S,NODE,,NTMP1,NTMP1+NRTUBE
NSEL,A,NODE,,NTMP2,NTMP2+NRTUBE
/OUT,%FNAME%.W_Data,out,,APPEND
/COM, Tube through-thickness stress at 0.5" below weld bottom
PRNS,COMP
/COM,
/COM, -----
/COM,
/OUT,
!
NSEL,S,NODE,,NNUM1,NNUM2
NSEL,A,NODE,,ncirc*10000+NNUM1,ncirc*10000+NNUM2
/OUT,%FNAME%.W_Data,out,,APPEND
/COM, Tube through-thickness stress at weld bottom
PRNS,COMP
/COM,
/COM, -----
/COM,
/OUT,
!
NSEL,S,NODE,,NNUM9,NNUM10
NSEL,A,NODE,,ncirc*10000+NNUM9,ncirc*10000+NNUM10
/OUT,%FNAME%.W_Data,out,,APPEND
/COM, Tube through-thickness stress at weld middle
PRNS,COMP
/COM,
/COM, -----
/COM,
/OUT,
```

Enclosure - Attachment 2

Document No.: C-7789-00-2

Revision No.: 1

Attachment Page: 3 of 6

```
!  
NSEL,S,NODE,,NNUM14,NNUM15,1  
NSEL,A,NODE,,ncirc*10000+NNUM14,ncirc*10000+NNUM15,1  
/OUT,%FNAME%.W_Data,out,,APPEND  
/COM, Tube through-thickness stress at weld top  
PRNS,COMP  
/COM,  
/COM, -----  
/COM,  
/OUT,  
!  
NSEL,ALL  
NTMP1=NODE (NX (1), NY (1), NZ (NNUM14)+0.5) ! Node 0.5" above downhill weld  
NTMP2=NODE (NX (ncirc*10000+1), NY (ncirc*10000+1), NZ (ncirc*10000+NNUM14)+0.5) ! Node 0.5"  
above uphill weld  
NSEL,S,NODE,,NTMP1,NTMP1+NRTUBE  
NSEL,A,NODE,,NTMP2,NTMP2+NRTUBE  
/OUT,%FNAME%.W_Data,out,,APPEND  
/COM, Tube through-thickness stress at 0.5" above weld top  
PRNS,COMP  
/COM,  
/COM, -----  
/COM,  
/OUT,  
!  
NSEL,S,NODE,,1,NNUM23,100  
NSEL,A,NODE,,ncirc*10000+1,ncirc*10000+NNUM23,100  
/OUT,%FNAME%.W_Data,out,,APPEND  
/COM, Tube ID stresses at uphill and downhill  
PRNS,COMP  
/COM,  
/COM,  
/COM, Location of ID nodes relative to tube bottom OD  
NLIST  
/OUT  
NSEL,S,NODE,,1+NRTUBE, NNUM23+NRTUBE,100  
NSEL,A,NODE,,ncirc*10000+1+NRTUBE,ncirc*10000+NNUM23+NRTUBE,100  
/OUT,%FNAME%.W_Data,out,,APPEND  
/COM,  
/COM,  
/COM, Tube OD stresses at uphill and downhill  
PRNS,COMP  
/COM,  
/COM,  
/COM, Location of OD nodes relative to tube bottom OD  
NLIST  
/COM,  
/COM, -----  
/COM,  
/OUT,  
!  
RSYS,SOLU  
NSEL,NONE  
NSEL,A,NODE,,NNUM14,NNUM15,1  
*REPEAT,ncirc+1,,,,10000,10000  
/OUT,%FNAME%.W_Data,out,,APPEND  
/COM, Tube stresses along plane opposite top of weld (Element-oriented CS)  
PRNS,COMP  
/COM,  
/COM, -----  
/COM,  
/OUT,  
!  
nset,all
```

```

esel,all
dsys,0
csys,11
!
/show,pscr
pscr,color,1
pscr,scale,.180
pscr,tranx,60
pscr,trans,200
pscr,rotate,0
!
*CREATE,WELDPLOT
/COM,
/COM, This macro makes tube stress plots with the geometry of the rest of
/COM, The model in the background. Use the following arguments for ARG1:
/COM,
/COM, ARG1 = 1 (hoop plot)
/COM, ARG1 = 2 (axial plot)
/COM, ARG1 = 3 (stress intensity plot)
/COM, ARG2 = results co-ordinate system (RSYS)
/COM,
/COM,
/COM, Set up for frontal view of model:
/VIEW,1,1
/ANG,1,VANG
/DIST,1,TW4*2.75*TOR
/FOCUS,1,-8.02,Y,SQRT(FILLETR**2-Y**2)
/DSC,1,OFF
ESEL,S,LIVE
NSLE ! Select tube nodes and elements
/TYPE,1,4
/EDGE,1,1 ! Alternate contours for stress plot
/PLOPTS,DEFA ! Standard legend
/PLOPTS,INFO,1 !!!!!!!!!!!!!!! Control style of EPLO
/COLOR,DEFA
/CVAL,1,-10000,0,10000,20000,30000,40000,50000,100000
/graphics,power ! ADDED THIS !!
avres,1 ! ADDED THIS !!
RSYS,ARG2
*IF,ARG1,EQ,1,THEN
  PLNS,S,Y ! Make hoop plot
*ELSEIF,ARG1,EQ,2,THEN
  PLNS,S,Z ! Make axial plot
*ELSE
  PLNS,S,INT ! Make stress intensity plot
*ENDIF
ESEL,ALL
NSEL,ALL

/graphics,full
*END
!
SET,,,,,T0+4.0
*USE,WELDPLOT,1,11
*USE,WELDPLOT,2,11
*USE,WELDPLOT,3,11
!
RSYS,SOLU
/pnum,type,1
/num,1
/color,num,blac,1
/view,1,-1
/type,1,4
/ang,1

```

Enclosure - Attachment 2

Document No.: C-7789-00-2

Revision No.: 1

Attachment Page: 5 of 6

```
/vup,1,z
/CVAL,1,-10000,0,10000,20000,30000,40000,50000,100000
!
/era
/auto
/edge,1
esel,s,mat,,1
nsle
*IF,THETA,LT,40.0,THEN
  /view,1,-1,,+1
*ELSE
  /view,1,-1,,+2
*ENDIF
/dsc,1,10
/type,1,4
pldi
/user
/noera
!
esel,all
!
esel,u,elem,,1,NNUM14-1
*repeat,ncirc,,,,10000,10000
esel,u,elem,,NNUM14+100,10000
*repeat,ncirc,,,,10000,10000
/edge,1,1
nsel,none
nsel,a,node,,nnum14,nnum15
*repeat,ncirc+1,,,,10000,10000
/type,1,0
plns,s,y
!
/era
/auto
/edge,1
esel,s,mat,,1
nsle
*IF,THETA,LT,40.0,THEN
  /view,1,-1,,+1
*ELSE
  /view,1,-1,,+2
*ENDIF
/dsc,1,10
/type,1,4
pldi
/user
/noera
!
esel,all
!
esel,u,elem,,1,NNUM14-1
*repeat,ncirc,,,,10000,10000
esel,u,elem,,NNUM14+100,10000
*repeat,ncirc,,,,10000,10000
/edge,1,1
nsel,none
nsel,a,node,,nnum14,nnum15
*repeat,ncirc+1,,,,10000,10000
/type,1,0
plns,s,z
!
/GRAPHICS,FULL
*CREATE,WELDTAB
  ESEL,S,LIVE
```

Attachment 2: File "Westpost8.txt"

Enclosure - Attachment 2

Document No.: C-7789-00-2

Revision No.: 1

Attachment Page: 6 of 6

```
NSLE
PRNS, S, COMP
NSEL, ALL
ESEL, ALL
*END
!
SET, , , , T0+4.0
RSYS, SOLU
/OUT, %FNAME%.results, txt
*USE, WELDTAB
/OUT, %FNAME%.nodelocs, txt
DSYS, 11

NLIST
/OUT
!
FINISH
/DELETE, WELDTAB
/DELETE, WELDPLT
FINISH
/exit, nosav
```